University of Nebraska - Lincoln
DigitalCommons@University of Nebraska - Lincoln

USGS Staff -- Published Research | US Geological Survey

2013

Some thoughts on the factors that controlled prehistoric maize production in the American Southwest with application to southwestern Colorado

Larry Benson
University of Colorado at Boulder, great.basin666@gmail.com

D. K. Ramsey
US Department of Agriculture-Natural Resources Conservation Service

David W. Stahle
University of Arkansas, dstahle@uark.edu

K. L. Peterson
University of Utah, ken.petersen@utah.edu

Follow this and additional works at: http://digitalcommons.unl.edu/usgsstaffpub

Benson, Larry; Ramsey, D. K.; Stahle, David W.; and Peterson, K. L., "Some thoughts on the factors that controlled prehistoric maize production in the American Southwest with application to southwestern Colorado" (2013). *USGS Staff -- Published Research*. 779.
http://digitalcommons.unl.edu/usgsstaffpub/779

This Article is brought to you for free and open access by the US Geological Survey at DigitalCommons@University of Nebraska - Lincoln. It has been accepted for inclusion in USGS Staff -- Published Research by an authorized administrator of DigitalCommons@University of Nebraska - Lincoln.

Journal of Archaeological Science 40 (2013) 2869–2880

Contents lists available at SciVerse ScienceDirect

Journal of Archaeological Science

journal homepage: http://www.elsevier.com/locate/jas

Some thoughts on the factors that controlled prehistoric maize production in the American Southwest with application to southwestern Colorado

L.V. Benson [a,*], D.K. Ramsey [b], D.W. Stahle [c], K.L. Petersen [d]

[a] Museum of Natural History, University of Colorado, 602 Pine St., Boulder, CO 80302, USA
[b] US Department of Agriculture-Natural Resources Conservation Service, 1281 County Rd 123, Hesperus, CO 813226, USA
[c] Department of Geosciences, University of Arkansas, Fayetteville, AR 72701, USA
[d] Geography Department, University of Utah, 260 Central Campus Drive, Room 270, Salt Lake City, UT 84112, USA

ARTICLE INFO

Article history:
Received 7 January 2013
Received in revised form
13 March 2013
Accepted 14 March 2013

Keywords:
Maize agriculture
Southwestern Colorado

ABSTRACT

In this paper, we present a model of prehistoric southwestern Colorado maize productivity. The model is based on a tree-ring reconstruction of water-year precipitation for Mesa Verde for the period A.D. 480 to 2011. Correlation of historic Mesa Verde precipitation with historic precipitation at 11 other weather stations enabled the construction of an elevation-dependent precipitation function. Prehistoric water-year precipitation values for Mesa Verde together with the elevation-dependent precipitation function allowed construction of the elevation of southwest Colorado precipitation contours for each year since A.D. 480, including the 30-cm contour, which represents the minimum amount of precipitation necessary for the production of maize and the 50-cm contour, which represents the optimum amount of precipitation necessary for the production of maize. In this paper, calculations of prehistoric maize productivity and field life for any specific elevation are also demonstrated. These calculations were performed using organic nitrogen measurements made on seven southwestern Colorado soil groups together with values of reconstructed water-year precipitation and estimations of the organic nitrogen mineralization rate.

Published by Elsevier Ltd.

1. Introduction

1.1. Study objectives

In this study we introduce an alternative model of prehistoric maize productivity for southwestern Colorado that can be used to supplement existing models of maize productivity and (or) provide an alternative approach to the calculation of maize yield and field life. Simple calculations of the effects of changes in water-year precipitation and soil organic-nitrogen (org-N) concentrations are performed in order to illustrate their effects on maize yields. In particular, the elevations of the minimum (30 cm) and optimum (50 cm) water-year precipitation contours are calculated for the period A.D. 600 to 1350. However, full-scale modeling of prehistoric maize productivity for southwestern Colorado is not attempted.

1.2. Previous studies and approaches

Several investigators (e.g., Burns, 1983; Petersen, 1994; Van West, 1994) have attempted to model prehistoric maize productivity for southwestern Colorado. More recently, Kohler (2012) extended and refined the approach of Van West (1994) as part of the Village Ecodynamics Project (VEP) (Kohler et al., 2012). Kohler's (2012) maize production model consists essentially of two parts: normalization of historic bean and maize yields and the application of tree-ring-based reconstructions of two climate variables – temperature and the Palmer Drought Severity Index (PDSI) – to estimate prehistoric maize yields from soils of southwestern Colorado. An outline and critique of the existing VEP maize productivity model is given in Supplementary Appendix 1.

Kohler's (2012) maize productivity model is complex and remarkably complete in its attempt to cover all processes impacting maize productivity; however, some of the model's parameterizations are somewhat problematic. We suggest that the VEP productivity model has two principal weaknesses, its application of National Resources Conservation Service (NRCS) values of available water capacity (AWC) and normal-year dry-weight productivity (NYDWP) in a number of parameterizations and its use of two remote high-elevation Bristlecone Pine ring-width series as temperature proxies for the growing season of maize. Problems with these parameterizations and applications are also discussed in Supplementary Appendix 1.

* Corresponding author. Tel.: +1 303 4495529.
E-mail address: lbenson@usgs.gov (L.V. Benson).

0305-4403/$ – see front matter Published by Elsevier Ltd.
http://dx.doi.org/10.1016/j.jas.2013.03.013

This article is a U.S. government work, and is not subject to copyright in the United States.

2. A different approach to the modeling of maize productivity

In this paper, we introduce a somewhat less complicated and, arguably, less parameterized approach to modeling maize productivity in southwestern Colorado. Four key factors control maize productivity: soil moisture, soil chemistry, soil texture, and solar insolation. Precipitation and its subsequent infiltration increase soil moisture. Solar insolation drives both evaporation and evapotranspiration which decrease soil moisture. Solar insolation also provides the energy for plant photosynthesis. Soil moisture and temperature control the mineralization of org-N to nitrate (NO_3^-), which is taken up by the roots of maize and incorporated in the growing plant. Soil textures in the Southwest can be broadly divided into two categories: fine sands and silts that promote precipitation infiltration and clay-rich soils that slow infiltration and that resist the adsorption of soil moisture by roots. Although there are a variety of other chemical parameters that affect soil productivity (e.g., pH, P, Fe, salinity), a soil's org-N concentration is arguably the most important measure of productivity. It should be noted, however, that elevated soil salinity can completely shut down the growth of maize (Ayers, 1977).

2.1. Estimation of prehistoric precipitation in southwestern Colorado

To estimate prehistoric precipitation, we first correlated standardized and detrended tree-ring indices of Mesa Verde Douglas fir to historical measurements (1949–2011) of Mesa Verde precipitation to define the seasonal precipitation response of the tree-ring data. The annual ring-width chronology is significantly correlated with precipitation during most months of the water year, so the tree-ring data were calibrated with water-year precipitation from 1949 to 2008. Precipitation data recorded prior to the calibration period were used for validation analysis of the reconstructions (the calibration and verification results are reviewed in Supplementary Appendix 2).

We used the tree-ring calibration to reconstruct Mesa Verde precipitation rates for the period A.D. 600–1300 (Fig. 1; Supplementary Table 1). We then created an elevation-dependent precipitation function (Fig. 2) using data from 11 other southwestern Colorado weather stations (Table 1) whose locations are shown in Supplementary Fig. 1. Water-year precipitation data for the period 1964 to 1986 (when water-year data for all 12 weather stations was available) were used to construct Fig. 2. Supplementary Fig. 2 shows the correlation of water-year precipitation at Mesa Verde and the other weather stations. All weather station data in this paper were taken from the Western Regional Climate Center's (2012) web page. The reconstructed prehistoric precipitation estimates can be used to calculate water-year precipitation values for any elevation in the study area during the prehistoric period, and the annual precipitation data can be used to screen for years of potential crop failure.

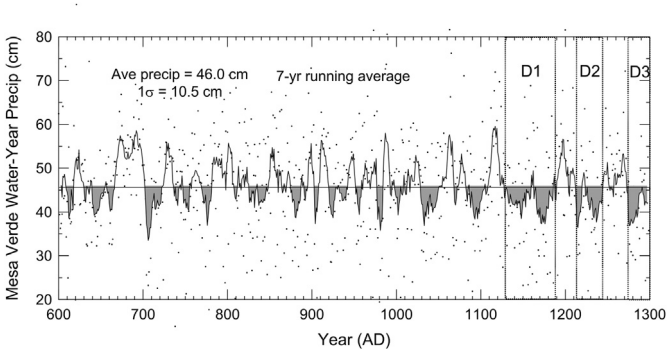

Fig. 1. Reconstructed Mesa Verde precipitation for the period A.D. 600–1300. Vertical rectangles within the 7-yr running average indicate times of relative drought. Major intense droughts are labeled D1, D2, and D3. D1 and D3 represent, respectively the middle 12th and late-13th century megadroughts that affected the Anasazi of southwestern Colorado. Megadroughts differ from other extended periods of dryness in that they lasted from 22 to 48 years and contained within them several consecutive-year dry periods, ranging from two to six years (Benson and Berry, 2009). Extended wet periods are associated with periods of intense construction activity and extended dry periods are associated with periods of little or no construction activity.

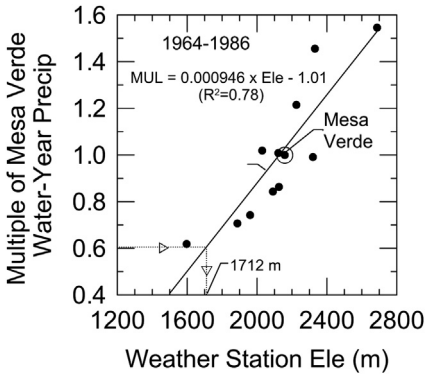

Fig. 2. Elevation dependence of water-year precipitation at 11 southwestern Colorado weather stations relative to Mesa Verde water-year precipitation. The mean value of precipitation between 1964 and 1986 for each station is plotted as a black dot.

Inline Supplementary Table S1 can be found online at http://dx.doi.org/10.1016/j.jas.2013.03.013.

Inline Supplementary Figs. S1 and S2 can be found online at http://dx.doi.org/10.1016/j.jas.2013.03.013.

A summer rainfall of ~15 cm and an annual precipitation of ~30 cm represent the lower limits for dry-land (rain-on-field) maize production in the northern hemisphere (Shaw, 1988). With regard to regions near the study area, Leonard et al. (1940) observed that crop failures in Colorado usually occurred when annual rainfall was <35 cm, and Jenkins (1941) suggested that precipitation of ~20 cm during June, July, and August marked the western limit of maize production in the United States. Thus, for every field site at a particular elevation at a particular time, annual values of precipitation <30 cm can be used to set maize yields to zero. It should be noted that ordinary water use by maize ranges from 41 to 64 cm (Hanway, 1966); thus values below 40 cm are probably indicative of times of moisture stress in southwestern Colorado, where the warm-season bare-soil evaporation rate is extremely high.

Mesa Verde's water-year precipitation has averaged 47.8 ± 10.6 cm for the period 1964–1986. Although the fit value (49.3 cm, Fig. 2) is slightly larger than 47.8 cm, we elected to use the fitted value when evaluating relative changes in precipitation as a function of elevation.

Table 1
Multiples of Mesa Verde precipitation and water-year statistics.

Weather station (m)		Water yr	Annual yr	Jun–Sep	Water yr (cm)	
		(1964–1986)	All data	All data	(1964–1986)	1σ
Hovenweep	1597	0.62	0.59	0.54	29.6	9.6
Cortez	1888	0.71	0.69	0.73	33.8	9.1
Ignacio	1960	0.74	0.78	0.87	35.5	9.0
Durango	2030	1.02	1.03	1.09	48.7	12.2
Yellow Jacket	2091	0.84	0.85	0.85	40.3	9.7
Dolores	2121	1.01	1.01	0.90	48.2	13.0
Mancos	2126	0.86	0.88	0.94	41.3	10.2
Mesa Verde	2159	1.00	1.00	1.00	47.8	10.6
Tacoma	2225	1.22	1.18	1.38	58.1	10.9
Fort Lewis	2320	0.99	0.98	1.07	47.4	11.1
Vallecito Dam	2332	1.46	1.46	1.60	69.6	17.1
Rico	2687	1.55	1.45	1.50	73.9	14.9

A 30-cm precipitation minimum represents a (30/49.3) = 0.61 multiple of Mesa Verde's average precipitation, which implies that maize could not have been grown below 1712 m during much of the historical period (Fig. 2). Actually, the data often fall outside the linear fit by ±150 m, indicating the approximate error in the calculation. Crop insurance for dry-land farming is not issued for elevations below 1830 m (Petersen, 1987b), which suggests that the lower elevation for historic maize production may be ~120 m higher than the value calculated using the linear fit displayed in Fig. 2 or that the insurance companies are erring on the side of caution by taking into account exceptionally dry years that occurred in the historical record. Obviously there is a great deal of variability in precipitation at any elevation from year to year (Fig. 3); thus, the dependence of precipitation on elevation for any particular water year will not be the same as the dependence of mean values of water-year precipitation with elevation as shown by the fit line in Fig. 2. However, for the purposes of this paper, we will assume that the linear regression depicted in Fig. 2 represents a fairly robust approximation of water-year precipitation for any particular elevation relative to the amount of precipitation measured at mesa Verde and that this relation allows us to approximate the relative movement of the 30- and 50-cm precipitation contours over the period A.D. 600 to 1350.

2.2. Grouping of soil types

The Cortez Soil Survey area consists of 152 mappable units, covering the area from the deserts of the Four Corners at ~1220 m to the Ponderosa Pine forest along the Dolores River Canyon at 2600 m (Ramsey, 1997). We aggregated the 152 soils (Supplementary Table 2) into 12 groups based on similar soil and environmental parameters. Seven of the groups were deemed suitable for maize production and five were considered unsuitable for farming (Table 2). Supplementary Fig. 1 shows the locations of the 12 grouped soils in the study area and Supplementary Fig. 3 shows the vegetation types that populate the seven productive soils.

Inline Supplementary Table S2 can be found online at http://dx.doi.org/10.1016/j.jas.2013.03.013.

Inline Supplementary Fig. S3 can be found online at http://dx.doi.org/10.1016/j.jas.2013.03.013.

2.3. The org-N content of the seven soil groups

As mentioned in the previous section, only seven of the 12 soil groups were considered productive in terms of dry-land maize farming. Our procedure considers org-N and its mineralization rate as two of four principal arbiters of maize productivity. To implement this concept, in September of 2011, we collected the upper 50 cm of a set (n ~30) of soil samples from each of the 7 soil groups. Soil samples referenced in this paper also were taken from Mesa Verde, Bandelier, and other areas in and around the San Juan Basin. The latter soil samples were collected from two depth ranges, 10–26 and 40–46 cm (Benson, 2010a). Locations of samples were obtained using a handheld GPS, usually accurate to <5 m. Samples were oven dried and the dried sample was disaggregated using a mortar and pestle. The disaggregated soil was then passed through a 2-mm screen and all particles >2 mm were discarded. The screened sample was homogenized by passing the sample five times through a riffle-type sample splitter. Total carbon (TC) (data not reported) and total nitrogen (TN) were determined on ~2 mg of ground sample, using an Exeter Analytical Model CE-440 rapid analysis elemental analyzer. The TN value should be considered

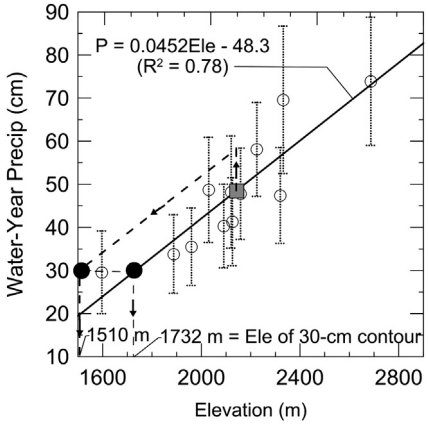

Fig. 3. Water-year precipitation as a function of elevation for 12 weather stations in southwestern Colorado. Error bars indicate ±1σ variation in precipitation at a particular station. Heavy dashed line with arrows indicates the effect of increasing precipitation by 10 cm on the elevation of 30-cm precipitation contour; i.e., it shifts from an elevation of 1732 to 1510 m (see text for further discussion).

Table 2
Grouping of southwest Colorado soils.

Soils suitable for farming

CE: Cool eolian soils. These soils are located at the higher elevations along the Dolores River canyon rim. They are formed mainly from eolian material with some input from local residual materials. Due to the natural sorting of the eolian material, and increased precipitation due to elevation, these soils tend to be higher in clay content than the soils at lower elevations that are closer to the source of the eolian material. The soils are generally deep to very deep with some area of stone content. Vegetation is mainly Gambels oak and ponderosa pine.

DE: Deep eolian soils. These soils are located across the mesa tops and uplands of the survey area. They are extensive and are the sites of current agricultural. They are moderately deep to very deep and generally free of any stones. These soils tend to have high concentrations of very fine sand and silt and have high water holding capacity. They extend from lower elevations around Hovenweep National Monument up to about 2290 m. They lie beneath the pinion and juniper forest and the sagebrush covered mesas.

CL: Clay soils derived from the Mancos Shale. These soils are located near the town of Mancos and extend west to near the entrance to Mesa Verde National Park. These soils are deep to very deep and developed in clayey alluvium from the Mancos shale and occur on fans below shale hills. Vegetation is generally composed of big sagebrush with pinion and juniper along the edges and on adjoining clay hills.

AL: Alluvial soils. These soils are a mixture of eolian material and alluvium from sandstone and shale. These soils tend to be sandy to loamy and occur in narrow swales and along narrow streams. Most of these areas do not have perennial streams but may receive water during spring snow melt or heavy thunderstorms. The alluvial soils are scattered throughout the mesas and valleys. Vegetation is mainly big sagebrush with areas of greasewood and four wing saltbush.

FN: Soils on alluvial fans. These soils are located along the toe slope of Mesa Verde near the entrance of the park and extending around the mesa past Towaoc. These soils are very deep, stratified, and loamy textured. They have uniform slopes and few stones larger than gravel. Vegetation consists mainly of big sage.

MVL: Eolian soils of Mesa Verde. These soils are moderately deep and to very deep eolian soils on the top of Mesa Verde. Because of the increased precipitation and longer growing season at these elevations, these soils were identified to have greater agricultural potential than other similar soils in the region. These soils have high water holding capacity and silt loam to clay loam textures.

CAL: Alluvial soils of Mesa Verde. These soils are located in the upper reaches of the major valleys that transect Mesa Verde. They are deep to very deep, well developed soils that have higher levels of organic material than most other alluvial soils. They are sites of increased precipitation and, in some settings, contain seasonal water tables.

Soils unsuitable for farming

ST: Steep soils of various parent materials

DR: Desert soils not suitable for farming

MC: Miscellaneous areas, dams, rock outcrop, water

SH: Shallow soils to bedrock

ED: Dry eolian soils of the desert.

equivalent to the total org-N value of a soil. The org-N data resulting from this study is listed in Supplementary Table 3 and summarized in Table 3.

Inline Supplementary Table S3 can be found online at http://dx.doi.org/10.1016/j.jas.2013.03.013.

2.4. Org-N and maize yields

As discussed in Benson (2010b), the modern above-ground maize plant contains 3.3 g N, and its root mass contains 0.4 g N; therefore, hills containing 2, 4, and 5 stalks of maize need, respectively, 7.4, 14.8, and 18.5 g of N in the form of NO_3^-. The NO_3^- is produced by the mineralization of org-N within the soil. The NO_3^- is highly mobile and is rapidly lost from the soil whether the plant absorbs it or not. Thus, once a field is cleared for planting, org-N will continually mineralize to NO_3^- and will be irreversibly lost from the soil zone. Elevated temperatures increase the activity of the microbial community in relatively wet regions, increasing the mineralization rate of org-N; however, in semiarid climates, increasing temperature dries the soil and reduces the decomposition rate of org-N. Greater soil moisture also translates into enhanced rates of microbial activity (Hoeft and Peck, 2002; Williams et al., 2000) and, therefore, increased mineralization rates. Thus the mineralization of org-N is both a function of temperature and precipitation.

A substantial amount of the org-N within the soil zone is not amenable to rapid mineralization. For example, Soudi et al. (1990) measured relative organic-N mineralization rates of eight semiarid Moroccan soils as a function of depth. The data indicate an exponential decrease in organic-N mineralization rate with depth and demonstrate that most of the org-N mineralization occurred within the upper 20–30 cm of the soil profile in semi-arid regions.

Data on the non-hydrolyzable component of Southwestern U.S. soils is lacking; however, data for other regions in North America suggest that approximately 50% of the upper 30–50 cm of North America soils is recalcitrant to mineralization (Table 5 in Benson, 2010b). Given the low amounts of mineralizable org-N below 50 cm (see Fig. 7 in Benson, 2010b) we make the assumption that only 50% of the total org-N in the upper 50 cm of Southwestern fields is susceptible to mineralization.

Maize root-length density, mass, and volume decrease exponentially with depth (Dwyer et al., 1996; Fehrenbacher and Rust, 1956; Qin et al., 2006). The root volume expands and deepens with time; i.e., root-length density contours descend relatively slowly over a 16-week growing period, with the roots reaching a depth of ~1 m. The upper near-surface root-ball radii of some types of modern hybrid maize extend 1.2 m outward from the stalk (Weaver, 1926). If most of the roots of maize are confined to the upper half meter of the root cone, we can approximate the overall volume of the root mass by a frustum with radii of 0.6 and 1.2 m, a height of 0.5 m, and a volume of 1.32 m^3. It is within this volume that NO_3^- becomes available to the maize plant and at a 100% efficiency of NO_3^- adsorption, 7.4, 14.8, and 18.5 g of NO_3^- must be produced to create hills containing, respectively, 2, 4, and 5 stalks of maize.

2.5. Organic-N mineralization rates

Soil organic matter (SOM) mineralization rates, usually refer to measurements of change in the organic carbon (org-C) component of the soil; however, as Herrmann (2003) has pointed out "Gross nitrogen mineralization is proportional to C mineralization in soils, so that C mineralization may be used as a predictor for gross N mineralization."

The following equation can be used to calculate k (the org-N or C mineralization rate constant) where t is the time (yr) elapsed between measurements of soil org-C; i.e., the time between measurement of C_o and C.

$$\ln\left[\frac{C}{C_o}\right] \Big/ t = k$$

Field studies in which the loss of org-N or C was measured over time from soils at a variety of sites indicate a range in k of 0.6–2.2%/yr (Table 4). Unfortunately, these sites are not representative of the study area in that the climates of the experimental sites are generally wetter and usually warmer than semi-arid southwestern Colorado. Thus, the calculated k values usually exceed the long-term k values for SOM and org-N in the Colorado study area.

2.6. The effect of solar radiation on maize yields

2.6.1. Growing degree and freeze-free days

The most common proxy for solar radiation in agriculture is growing degree days (GDD), defined as

$$\mathrm{GDD} = \left[\left(T_{\mathrm{high}} + T_{\mathrm{low}}\right)/2\right] - 10$$

in which T_{low} and T_{high} are the daily high and low temperatures (°C), and T_{high} is capped at 30 °C. Generally high (1330–1780) GDD are necessary for optimal crop yields in the Midwest where high humidity suppresses transpiration and soil evaporation; however, high GDD can negatively affect maize yields in the Southwest. For example, Petersen (1987a) found that, between 1920 and 1960, yields of dry-land maize grown in Dolores and Montezuma Counties, Colorado, were negatively related to GDD values measured at the Yellow Jacket weather station. Whereas increases in solar radiation may promote photosynthetic activity, solar radiation also increases transpiration and evaporation of soil moisture, which causes the plant to wilt. In addition, if air temperature exceeds 32 °C, maize begins to stress during pollination and grainfill (Thomison et al., 2012) and temperatures in excess of 38 °C may actually kill maize pollen (Nielson, 2012). Both processes resulted in massive crop failures in the American Midwest during the summer of 2012. Petersen (1987a) demonstrated that maize could be grown under warm (~1400 GDD) conditions, if annual precipitation was elevated (46 cm), and that maize could be grown under relatively dry conditions (as little as 33 cm of precipitation) if the climate was cool (~900 GDD). Bellorado (2007) demonstrated excellent yields of Hopi Blue maize in 2004 when GDD ranged between 970 and 1100 GDD at elevations ranging from 2070 to 2105 m in the Ridges

Table 3
Quartile and mean total *N* values of study area soils.

	Morefield valley Alluvium	Mesa Verde Alluvial fan	SW CO cool Eolian	SW CO Clay	Zuni field Soils	SW CO Alluvial	Chapin mesa Loess	Bandelier Soils	SW CO deep Eolian Loess	Wetherill mesa Loess	Chaco corridor Soils	Hopi dune Field
1st quartile	0.101	0.095	0.090	0.075	0.058	0.052	0.056	0.034	0.037	0.037	0.028	0.006
2nd quartile	0.116	0.107	0.098	0.080	0.073	0.071	0.070	0.057	0.053	0.046	0.044	0.013
3rd quartile	0.169	0.116	0.110	0.099	0.093	0.093	0.083	0.061	0.069	0.054	0.070	0.036
Mean	0.141	0.109	0.099	0.085	0.077	0.074	0.079	0.050	0.054	0.048	0.050	0.020

Table 4
Field-based soil organic matter mineralization rates.

Area	Years	Plants	N_{org} Min. Rate	Reference
Rothamsted, England	100	None	0.59%/yr	Jenkinson and Rayner (1977)
Nebraska	22	No-till wheat	0.60%/yr	Doran et al. (1998)
Minnesota	9	None	0.69%/yr	Clay et al. (2007)
Nebraska	22	No-till wheat	0.78%/yr	Doran et al. (1998)
Minnesota	13	None	1.18%/yr	Clay et al. (2007)
South Dakota	5	None	2.21%/yr	Clay et al. (2007)

Basin area southwest of Durango, Colorado. When GDD fell below a value of 910, maize yields declined precipitously.

Another measure of solar radiation is the length of the freeze-free growing season. Most varieties of maize, including Southwest Native American landraces such as Hopi blue maize and a variety of Zuni cultivars, require about 120 freeze-free days (FFD) (e.g., Bradfield, 1971; Muenchrath et al., 2002). The 120 days refers to the time from emergence to black-layer formation which indicates physiological maturity of the maize plant. In the case of the of Hopi Blue maize grown by Bellorado (2007), good yields occurred when the length of the freeze-free period exceeded 117 days. When FFD fell to ≤115 days, yields markedly decreased. Supplementary Table 4 which lists the 90% probability of FFD between 0 °C in spring and autumn as well as the probability of a site reaching 120 FFD during summer, indicates that there is a very complicated relationship between FDD and elevation in southwest Colorado. Note that the probability of achieving >115 FFD is high for Cortez (94%), Mesa Verde (92%), and Yellow Jacket (88%), but is very low for Rico (0%), Vallecito (21%), Ignacio (22%) and Durango (36%). This suggests that the latter four sites represent elevations and/or topographies inimical to maize farming during relatively warm times.

Inline Supplementary Table S4 can be found online at http://dx.doi.org/10.1016/j.jas.2013.03.013.

Optimally, we would like to include the effects of both GDD and FFD in our model of maize productivity. Unfortunately, there is also no simple relationship between GDD and elevation for the eight southwestern Colorado weather stations that record GDD (Fig. 4B), although there is an excellent relationship between both and summer (JJAS) and mean-annual temperatures and GDD (Fig. 4C, D; see Supplementary Table 4 for temperature and GDD statistics). Even if there were a simple relationship between elevation and historic GDD, we still need to reconstruct prehistoric values of GDD, which implies we need to find a proxy for southwest Colorado prehistoric temperatures.

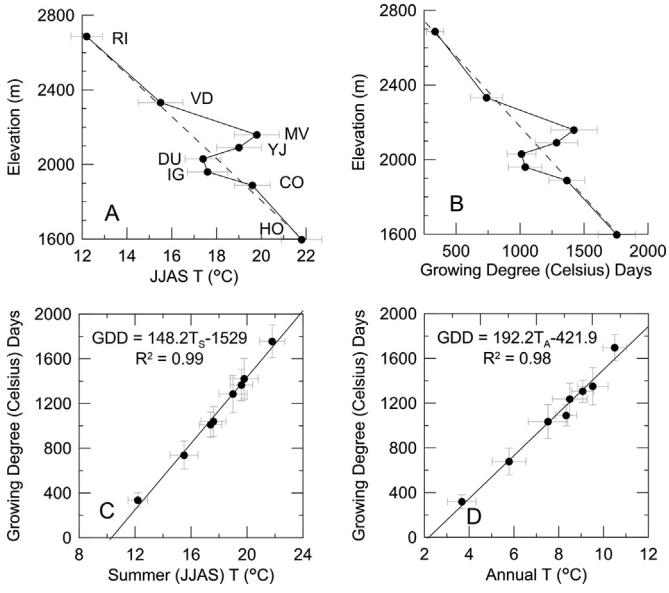

Fig. 4. A. Summer (JJAS) mean temperatures and B. growing degree days (GDD) at Rico (RI), Vallecito Dam (VD), Mesa Verde (MV), Yellow Jacket (YJ), Durango (DU), Ignacio (IG), Cortez (CO), and Hovenweep (HO) weather stations plotted as a function of elevation. GDD plotted as a function of C. summer and D. annual mean temperatures.

2.6.2. *Bristlecone Pine ring width as a proxy for prehistoric summer temperatures*

Kohler (2012) indicated some success linking prior- and current-year September temperatures at Mesa Verde and Yellow Jacket weather stations with Bristlecone Pine ring widths at Almagre. He also was able to correlate the 1st principal component of the combined Almagre and San Francisco Peaks ring-width series to September temperatures at these two sites.

We reassessed the ability of Bristlecone Pine ring widths to reconstruct prehistoric temperatures by regressing June, July, August, and September temperatures, mean summer (JJAS) temperatures, and GDD values for each of eight weather stations against both current and prior-year ring widths of Bristlecone Pines from Almagre, Colorado (updated data set provided by Connie Woodhouse) and San Francisco Peaks, Arizona (data provided by Matthew Salzer; see also Salzer and Kipfmueller, 2005). With regard to the Almagre record, data from all eight weather stations were regressed against prewhitened standardized and detrended ring widths of Almagre Bristlecone Pine. Data from Mesa Verde and Yellow Jacket weather stations were also regressed against standardized and detrended ring widths of Almagre Bristlecone Pine that had not been prewhitened in order to determine if prewhitening negatively affected the correlations.

Of the 266 regressions, only 7 explained at least 20% of the variance of the independent thermal variable (Table 5), with most of those regressions associated with the Yellow Jacket weather station. Obviously, the locations of some of the weather stations (e.g., Rico, Vallecito Dam, Ignacio, and Durango) are outside the VEP study area; however, these sites provide data useful in determining whether growing season proxies at these elevations can be linked to high-elevation Bristlecone ring widths.

Many of the temperature and GDD correlations were *negatively* related to ring width, with decreasing temperatures associated with increasing ring widths (see; e.g., Fig. 5). San Francisco Peaks Bristlecone Pine ring widths failed to explain more than a few tenths of a percent of the variances in summer temperatures and GDD measured at the nearby Fort Valley weather station (Table 5), illustrating the inherent inability of the San Francisco Peaks tree-ring record to predict growing season temperature variability. Correlations of FFD with the tree-ring records did not fare any better (Table 5). The results of these regressions suggest that, at this time, there does not exist any objective way of using high-elevation tree rings to reconstruct high-frequency (annual) prehistoric proxy records of the summer growing season in southwestern Colorado.

Instead of using tree-ring widths, it may be possible to use tree-ring densities of high-elevation Bristlecone Pine to estimate prehistoric changes in southwest Colorado temperatures. For example, Briffa et al. (2001) have used this method to reconstruct a composite proxy-temperature series of Northern Hemisphere temperatures for the past 600 years.

2.6.3. *Pollen-based reconstructions of low-frequency temperature and precipitation variability*

Petersen (1988) used pollen ratios from two sites Beef Pasture (3060 m) and Twin Lakes (3290 m) in the LaPlata Mountains ~25 km northwest of Durango, Colorado, to reconstruct relative changes in summer air temperature and winter precipitation for

Table 5
R^2 of temperature proxies versus Bristlecone pine ring widths.

Weather station	Jun *T*	Jul *T*	Aug *T*	Sep *T*	Ave JJAS *T*	GDD	FFD
Current-year T (celsius) proxy vs prewhitened Almagre standarized ring widths							
Mesa Verde	0.000	0.000	0.000	0.009	0.001	0.002	0.003
Hovenweep	0.013	0.015	0.010	0.002	0.007	0.001	0.024
Cortez	0.000	0.009	0.003	0.005	0.000	0.005	0.001
Ignacio	0.005	0.002	0.034	0.019	0.027	0.018	0.028
Durango	0.004	0.014	0.015	0.004	0.003	0.001	0.015
Yellow Jacket	0.000	0.129	0.038	0.007	0.000	0.000	0.015
Vallecito Dam	0.003	0.002	0.023	0.002	0.001	0.000	0.019
Rico	0.001	0.011	0.026	0.002	0.000	0.002	0.000
Current-year T (celsius) proxy vs San Francisco Peaks standarized ring widths							
Mesa Verde	0.106	0.025	0.014	0.007	0.026	0.051	0.038
Hovenweep	0.000	0.026	0.006	0.040	0.000	0.000	0.000
Cortez	0.000	0.013	0.022	0.020	0.011	0.023	0.040
Ignacio	0.004	0.000	0.035	0.006	0.006	0.003	0.061
Durango	0.082	0.050	**0.200**	0.052	0.148	0.134	0.007
Yellow Jacket	0.018	0.001	0.187	0.152	0.119	0.114	0.035
Vallecito Dam	0.000	0.075	0.006	0.002	0.007	0.014	0.018
Rico	0.013	0.000	0.019	0.026	0.025	0.023	0.008
Fort Valley	0.013	0.001	0.033	0.031	0.004	0.001	n.d.
Prior-year T (celsius) proxy vs prewhitened Almagre standarized ring widths							
Mesa Verde	0.002	0.010	0.041	0.031	0.022	0.000	0.008
Hovenweep	0.003	0.024	0.085	0.134	0.102	0.150	0.032
Cortez	0.001	0.077	0.097	0.100	0.090	0.055	0.051
Ignacio	0.000	0.030	0.009	0.045	0.027	0.025	0.014
Durango	0.000	0.069	0.084	0.056	0.039	0.032	0.019
Yellow Jacket	0.020	0.173	0.129	0.083	0.172	**0.220**	0.000
Vallecito Dam	0.008	0.064	0.030	0.033	0.025	0.023	0.002
Rico	0.003	0.075	0.041	0.087	0.088	0.114	0.004
Prior-year T (celsius) proxy vs San Francisco Peaks standarized ring widths							
Mesa Verde	0.044	0.034	0.028	0.011	0.018	0.027	0.014
Hovenweep	0.003	0.046	0.086	0.008	0.026	0.022	0.031
Cortez	0.013	0.027	0.007	0.011	0.006	0.010	0.072
Ignacio	0.027	0.000	0.011	0.014	0.009	0.006	0.051
Durango	0.177	0.074	0.086	0.066	0.194	0.155	0.000
Yellow Jacket	0.061	0.004	0.060	0.176	0.136	0.095	0.018
Vallecito Dam	0.009	0.057	0.026	0.000	0.005	0.009	0.089
Rico	0.023	0.054	0.034	0.010	0.002	0.001	0.004
Fort Valley	0.000	0.007	0.004	0.035	0.006	0.004	n.d.
Current-year T (celsius) proxy vs Almagre standarized ring widths not prewhitened							
Mesa Verde	0.002	0.078	0.079	0.109	0.104	0.074	0.012
Yellow Jacket	0.044	0.057	0.000	0.001	0.023	0.019	0.041
Prior-year T (celsius) proxy vs Almagre standarized ring widths not prewhitened							
Mesa Verde	0.005	0.016	0.005	0.011	0.012	0.066	0.000
Yellow Jacket	0.133	**0.279**	**0.251**	0.084	**0.353**	**0.344**	**0.024**

Bold numbers indicate correlations with $R^2 > 0.19$.

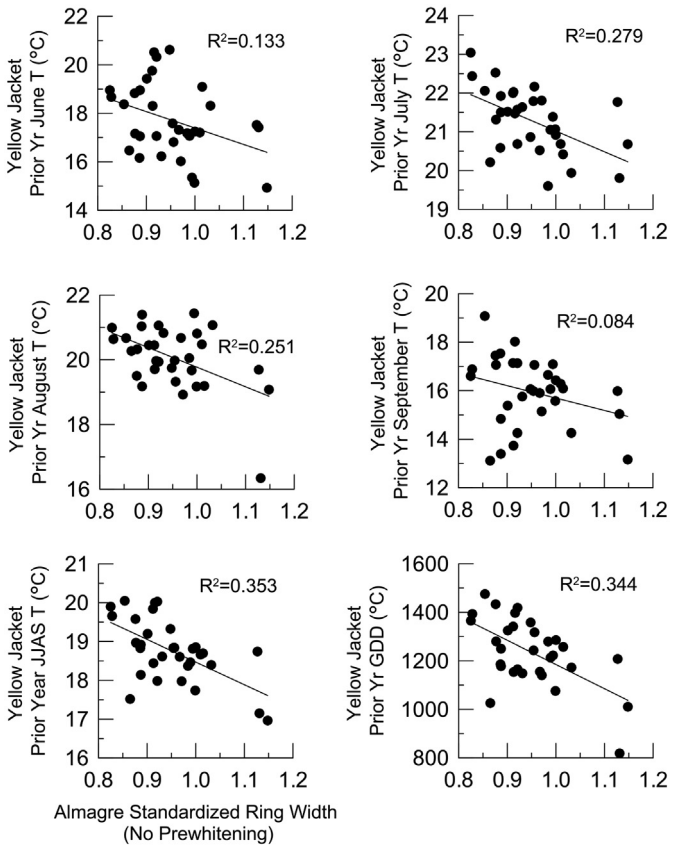

Fig. 5. Yellow Jacket prior-year June, July, August, September, summer (JJAS) temperatures and GDD plotted as a function of Almagre Bristlecone Pine standardized ring widths with no prewhitening of the data. Note that the correlations are negative; i.e., decreasing temperatures occur with increasing ring width, a pattern that makes little sense if tree growth responded positively to warming.

the past several thousand years. Conifer/non-arboreal pollen (NAP) ratios from the Twin Lakes site, today situated ~250 m below the upper elevation limit of *Picea*, were used to provide a record of past summer temperatures derived from changes in the elevation of the temperature sensitive upper tree line and spruce/pine ratios from the Beef Pasture site were used to create an index of winter precipitation.

Wright (2012) recently recored Beef Pasture creating a high-resolution pollen record for the past 2300 years that was constrained by 16 calibrated AMS ^{14}C samples. Wright (2012) used spruce/*Pinus ponderosa* and sedge/Cheno-am ratios from the Beef Pasture pollen record in an attempt to create low-frequency proxy records of, respectively, temperature and precipitation at this site. Thus Wright (2012) and Petersen (1988) derive two different measures from essentially the same spruce to pine ratio: Wright (2012) derived only temperature, while Petersen (1988) derived effective soil moisture (primarily from winter precipitation). For his winter precipitation measure, Wright (2012) uses the sedge/Cheno-am ratios. Unfortunately, sedge is not evenly distributed across the landscape and major changes in sedge percentages occur over short distances; e.g., even though Petersen's (1988) and Wright's (2012) coring sites were only meters apart, the cores contained drastically differing amounts of sedge (compare Cyperaceae in Fig. 3.3 in Wright (2012) with Cyperaceae in Fig. 22 of Petersen (1988)). In addition, Petersen (1988) previously pointed out that increases in spruce pollen in Beef Pasture result from increases in effective soil moisture (a function of increased precipitation and colder temperatures), which is not an indicator of temperature alone as suggested by Wright (2012). Dix and Richards (1976) found that spruce predominates in environments where the snowpack persists longest resulting in greater soil moisture, an observation that supports Petersen's (1988) interpretation of the spruce/pine pollen ratio.

Petersen's (1988) pollen record is neither highly resolved nor is it precisely dated and Wright's (2012) temperature proxy is highly problematic. Thus, for the time being, we do not even have the means of constructing prehistoric low-frequency records of temperature variability, including FFD and GDD, as a function of elevation across southwest Colorado.

2.7. Model applications

2.7.1. Example calculations using the productivity model

In this example, we assume that 30 cm represents the minimum amount of water-year precipitation necessary for maize production. We also assume that a Native American family moves to an alluvial soil at an elevation of 1940 m in A.D. 1200 and clears a 1-

acre field. In the spring of A.D. 1201, the family plants 440 hills of maize, and selects the four best stalks in each hill after the stalks emerge. In water-year A.D. 1201, Mesa Verde received 51.7 cm of water-year precipitation (Supplementary Table 1). At 1940 m, the Native American field received 0.83 times the amount of Mesa Verde precipitation (using the linear fit in Fig. 2) or 43 cm. Thus, precipitation was close to optimum for maize production.

In order to determine if there is sufficient NO_3^- produced in the root frustum to produce 10 bu maize/ac, it is necessary to scale the org-N mineralization rate to the water-year precipitation amount. Given that most elevations over 2200 will have experienced abbreviated growing seasons in the past, we use values of reconstructed water-year precipitation at Mesa Verde to scale the org-N mineralization rate. Between A.D. 600 and 1300 Mesa Verde precipitation ranged from 13 to 89 cm and had mean and 1σ values of, respectively, 46 and 12 cm. We arbitrarily assign a 2.0%/yr mineralization rate to a 70-cm (2σ) water year and a 0.0%/yr mineralization rate to a 0-cm water year and further assume that the mineralization rate is a linear function of these two end members; e.g., a 35-cm water year would be associated with a 1.0%/yr mineralization rate.

The org-N mineralization rate at the 1940-m field is given by (43 cm/70 cm) × 2%/yr = 1.23%/yr. A random pick of org-N from the alluvial soils histogram (Fig. 6) yields a value of 0.05%, only half of which is labile and subject to mineralization. The 1.32 m^3 root frustum is assumed to have a density of 1.5 g/cm^3 (mean density of Montezuma County soils; National Resources Conservation Service, 2012). The frustum contains 1.32×10^6 $cm^3 \times 1.5$ g/$cm^3 = 1.98 \times 10^6$ g of soil. The soil volume in the frustum contains 1.98×10^6 g × 0.005/2 = 4950 g of mineralizable org N. Therefore, in A.D. 1201, 0.0123 × 4950 g = 60.9 g of NO_3^- is produced in the frustum which greatly exceeds the needed 14.8 g of NO_3^-. Therefore, the 1-acre field should yield 10 bu of maize.

In the following year (A.D. 1202), Mesa Verde receives 29.8 cm of precipitation (Supplementary Table 1) and the Native American field receives 24.7 cm of precipitation. Crop failure results because <30 cm of precipitation was received. However, we still need to keep track of org-N mineralization and its disappearance over time. The mineralization rate is relatively low (24.7 cm/70 cm × 2 %/yr = 0.71%/yr). The amount of org-N mineralized in A.D. 1202 is the amount of org-N remaining in the frustum after it's A.D. 1201 loss times its mineralization rate; i.e., (4950 g−60.9 g) × 0.0071 = 34.7 g of org N. So the bad news is that the crop failed during the dry year but the good news is that not much org-N was lost from the field.

We also need a means of calculating the useful life of an agricultural field. For the model, the precipitation and org-N mineralization calculations proceed until crop failure becomes routine. We define "useful field life" as the time span during which the amount of org-N in the root frustum is sufficient to support "*n*" stalks of maize. In our particular example, 14.8 g of NO_3^- are necessary to support a density of 4 stalks/hill. By keeping track of the residual org-N in the root frustum over time, one can also determine when the total org-N value is nearing its 14.8 g limiting value (given an average water year). At that time the field would be abandoned and the Native American family would choose a new field site.

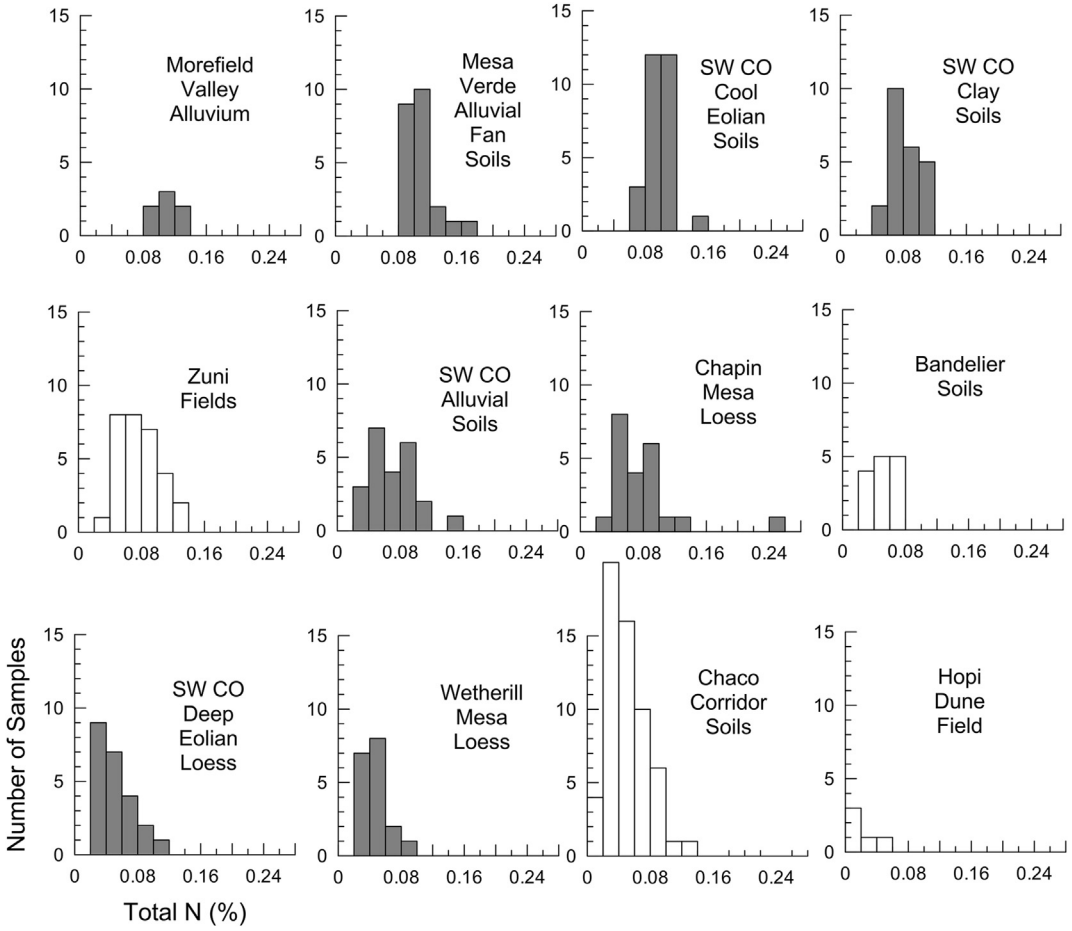

Fig. 6. Histograms of total N in the upper 50 cm of soils from southwestern Colorado, Hopi, Arizona, and from Chaco Canyon, the Zuni Reservation, and Bandelier National Park, New Mexico. Data from southwestern Colorado soils are shown as gray histograms.

2.7.2. Changes in the dry-land farming elevation band

Petersen (1988) previously estimated the low-frequency change in the upper and lower elevations of the prehistoric agricultural belt in southwest Colorado. Petersen (1988) equated historical pollen ratios (conifer/NAP pollen ratios at Twin Lakes and spruce/pine pollen ratios at Beef Pasture) with, respectively, the observed historic movement of timberline and lower elevation of the spruce forest. A rise in timberline can be associated with an increase in the 10 °C July isotherm (summer warmth), whereas an increase in the lower elevation of the spruce forest can be equated with a decrease in the winter snowpack. The modern farming belt that is sufficiently wet (35 cm of annual precipitation) and warm (110 FFD) for the growth of bean and maize is relatively narrow with elevational limits of 2010 and 2380 m in the Dolores area. Petersen (1988) estimated the prehistoric elevation and width of this belt by first comparing historic values of the spruce/pine and conifer/NAP ratios with the elevation limits of historic dry-land farming at certain times and then using prehistoric values of these ratios to approximate the elevation and width of the prehistoric farming belt. In the following, we present a new method for determining high-frequency (interannual) change in the lower elevation limit of prehistoric maize agriculture as well as the elevation of optimum prehistoric maize production in southwest Colorado.

The upper and lower limits of maize farming changed over time as a function of precipitation, FFD, and GDD. Unfortunately we are unable to approximate past values of the latter two parameters in this paper. However, a fit of water-year precipitation as a function of elevation (Fig. 3, Table 1) allows us to approximate the elevation of past water-year precipitation contours as a function of time.

We first calculate the present-day elevations of the 30- and 50-cm precipitation contours. In this calculation, the 30-cm contour represents the lower limit of precipitation necessary for the production of maize and the 50-cm contour represents the approximate optimum value of precipitation necessary for the production of maize. Substituting the two precipitation values in the linear fit depicted in Fig. 3 yields present-day elevations of 1732 and 2175 m, respectively, for the 30- and 50-cm contours.[1] These values indicate that for every 1-cm increase in precipitation, a particular precipitation contour decreases 22.2 m in elevation and vice versa. We then calculate the prehistoric annual elevations of the 30- and 50-cm contours given the historic Mesa Verde (MV) precipitation value of 49.3 cm and the reconstructed prehistoric Mesa Verde precipitation value, using the following three equations:

$$\text{Prehistoric MV precipitation} - 49.3\ \text{cm} = \text{N cm(past change in MV precipitation)}; \quad (1)$$

$$\text{If } N > 0,\ Y = N \times 22.2 \text{ and elevation of } 30-\text{cm contour} = 1732 - Y; \quad (2)$$

$$\text{If } N < 0,\ Y = N \times 22.2 \text{ and elevation of } 30-\text{cm contour} = 1732 + Y.; \quad (3)$$

To determine the elevation of the 50-cm precipitation contour, 2175 is substituted for 1732 in the previous equations.

Fig. 3 displays how the 30-cm precipitation contour changes in elevation with a 10-cm increase in Mesa Verde precipitation; i.e., the precipitation-elevation linear fit shifts vertically 10 cm along the precipitation axis and the intersection of the shifted line with the 30-cm precipitation value determines the new elevation of the 30-cm contour (1510 m).

In Figs. 7 and 8, the elevational limits of the Great Sage Plain (1500–2100 m) and the modern farming belt (2010–2380 m) have been bounded, respectively, by rectangles with dashed and solid lines. Some have suggested that the Great Sage Plain functioned as the "bread basket" of the Anasazi that inhabited southwestern Colorado. Fig. 7 depicts the elevation of the 30-cm water-year contour for the period A.D. 600 to 1350. The data enclosed in dark gray have been smoothed with a 3-yr running average. The thick white line represents a 21-yr running average of the data, which is used to outline persistent wet and dry phases of the record. Note the presence of the A.D. 1130–1180 (middle-12th century), and the A.D. 1276–1300 (late-13th century) droughts in the record. In general the Great Sage Plain would have produced some maize during 89% of the period of record. However, the mid-12th century megadrought was particularly intense with several years in which maize would have had to be grown above 2200 m, an elevation generally associated with a very short growing season.

The plot of the 50-cm water-year contour (Fig. 8) indicates, that during only 33% of the time, could an optimum crop of maize been produced within the elevational range of the Great Sage Plain and that 23% of the time the 50-cm contour lay above the upper elevation range of the modern dry-land farming belt.

The question arises "how would have prehistoric Native Americans responded to the interannual variability of precipitation?" Fig. 9 indicates the absolute value of the interannual difference in any precipitation contour for southwest Colorado between A.D. 600 and 1350. The mean and median values of the interannual change in elevation of a particular contour are, respectively, 287 and 231 m. Thus, more than 50% of the time, the elevation of the 30-cm precipitation contour would shift more than 231 m either up or down within a year. We suggest that, in general, it was difficult to predict either the direction or magnitude in the shift of annual precipitation. However, the depth and areal extent of winter snowpack might have been used as a rough indicator of spring soil moisture. In addition, successive series of anomalously wet or dry years might also have provided insight as to the probable lower elevation limit of agricultural productivity. However, to be on the safe side, Native Americans would have had to generally farm at upper elevations where agriculture was mostly limited by the length and intensity of

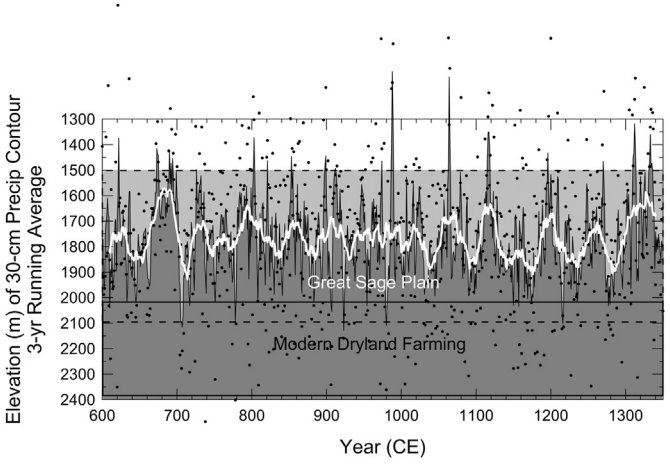

Fig. 7. Elevation of the 30-cm water-year precipitation contour for the period A.D. 600–1350. The data enclosed in dark gray have been smoothed with a 3-yr running average. The thick white line represents a 21-yr running average of the data, which is used to outline persistent wet and dry phases of the record. The Great Sage Plain lies between elevations of 1500 and 2100 m and the region of modern dry-land farming in the Dolores area lies between 2010 and 2380 m.

[1] Note that these elevations differ slightly from those calculated using the fit to weather station multiples of Mesa Verde precipitation shown in Fig. 2.

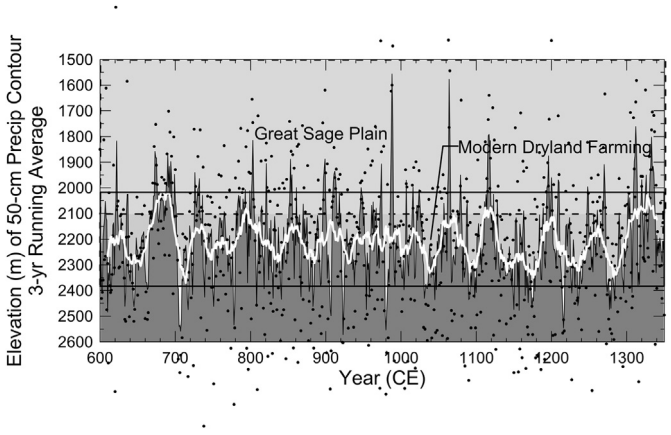

Fig. 8. Elevation of the 50-cm water-year precipitation contour for the period A.D. 600–1350. The data enclosed in dark gray have been smoothed with a 3-yr running average. The thick white line represents a 21-yr running average of the data, which is used to outline persistent wet and dry phases of the record. The Great Sage Plain lies between elevations of 1500 and 2100 m and the region of modern dry-land farming in the Dolores area lies between 2010 and 2380 m.

the summer growing season and (or) they would have had to scatter their fields over a range in elevations in response to the variability in interannual precipitation.

Petersen (1988) found that the tree line had risen during the past 150 years in the LaPlata Mountains, suggesting an increase in regional air temperature. If the past GDD profile during warm (dry) periods with elevation was similar to the present-day profile (Fig. 4B), elevations above 2200 m would have received <1000 GDD, a value that may represent the minimum for the production of maize. This suggests that, in general, elevations above 2200 m were not suitable for prehistoric agriculture during most of the time.

2.8. Future improvements to the model

2.8.1. Some limited ways of dealing with the effect of temperature on the growing season

At this point in time, it appears that the amount of heat impacting maize at any particular field site in southwestern Colorado is a complicated function of solar radiation and the topography of the landscape, which in some cases leads to the pooling of cold air (e.g., Ignacio, Colorado) and, in other situations, leads to increased levels of heating (e.g., Mesa Verde) (see Fig. 4). Present-day land-surface temperature and soil moisture measurements of southwestern Colorado could be obtained, using satellite-based instrumentation in combination with surface-based temperature and soil-moisture sensors (see, e.g., Holmes, et al., 2011). If such measurements were made using a sufficiently small grid area, they could be used to identify areas routinely impacted by cold air pooling. Those areas could then be ruled out as potential field sites.

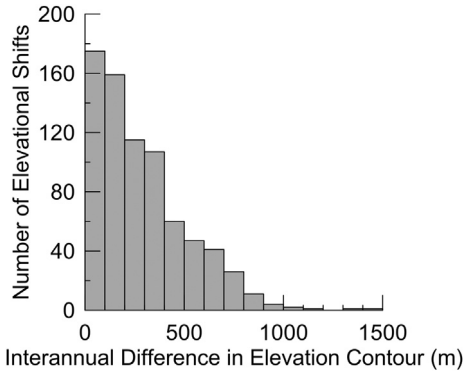

Fig. 9. Histogram depicting interannual shifts in the elevations of the 30-cm contour in southwestern Colorado.

We suggest that the upper boundary of present-day dry-land farming (2380 m) represents a maximum limit of maize production during prehistoric periods of relative warmth; e.g., most of the weather stations indicate a weak but negative association of GDD with water-year precipitation (Fig. 10). This suggests the upper limit of maize production fell during times of increased moisture availability. Given that most of the historical period (1919–1982) used to define the upper limit of the dry-land farming belt (Petersen, 1987a) was in drought (Fig. 11) and was substantially warmer on average (Petersen, 1988), we would expect the upper limit of maize production to have fallen below the 2380 m boundary during prehistoric wet periods.

2.8.2. Other potential low-frequency records of climate change

With respect to low-frequency records of climate change, shallow lakes suitable for pollen-based or other proxy temperature reconstructions exist not only in the Twin Lakes region northwest of Durango but also on the Mogollon Rim of the Colorado Plateau. For example, Anderson (1993) performed a low-resolution pollen study of sediments from Potato Lake, Arizona, where the upper 75 cm of sediment yielded a climate record for the past 3500 years. A 0.5-cm continuous sampling of the upper part of such a core would yield a 25-year resolution of late-prehistoric climate change.

A record of climate change for the past 2000 years is contained within the top 90 cm of sediment of Twin Lakes sediments (Petersen and Mehringer, 1976); thus, if another core was collected from this site and sampled continuously over 0.5-cm intervals, a 10-yr resolution of late-prehistoric climate change would result.

Although the use of alkenones to reconstruct past lake-water temperatures is still in its infancy (see, e.g., Theroux et al., 2010), it may, in the future, be possible to obtain prehistoric records of lake temperature change from some of the southwestern U.S. lakes. This organic marker has been successfully applied to marine sedimentary sequences (see, e.g., Barron et al., 2003).

2.8.3. Estimates of summer rainfall

One substantial parameter missing from our model is summer (monsoonal) precipitation. Griffin et al. (2011) and Meko and Baisan (2001) have demonstrated some success in using conifer latewood widths to retrodict past regional summer precipitation amounts and Leavitt et al. (2011) have shown that the carbon isotope content of tree rings also has potential in determining the strength of the summer monsoon in the American Southwest. Such studies would greatly benefit the understanding of prehistoric maize productivity in southwestern Colorado.

2.8.4. Tapering of maize yields with reductions in precipitation and available NO_3^-

In our model, total crop loss occurred when there was <30 cm of water-year precipitation and <14.8 g NO_3^- produced in the root frustum (4-stalk condition). When these limiting values were met or exceeded, 10 bu/ac of maize was produced. In reality, nutrient and water stress probably begins to take effect prior to the limiting value is reached. One way to deal with this would be to produce yield functions that decrease with decreasing water-year precipitation and NO_3^- produced in the root frustum. Fig. 12A and B illustrate examples of such functions. Response of maize yields to precipitation and to loss of org-N could be provided via experimental maize gardens that were cultivated for two or more decades.

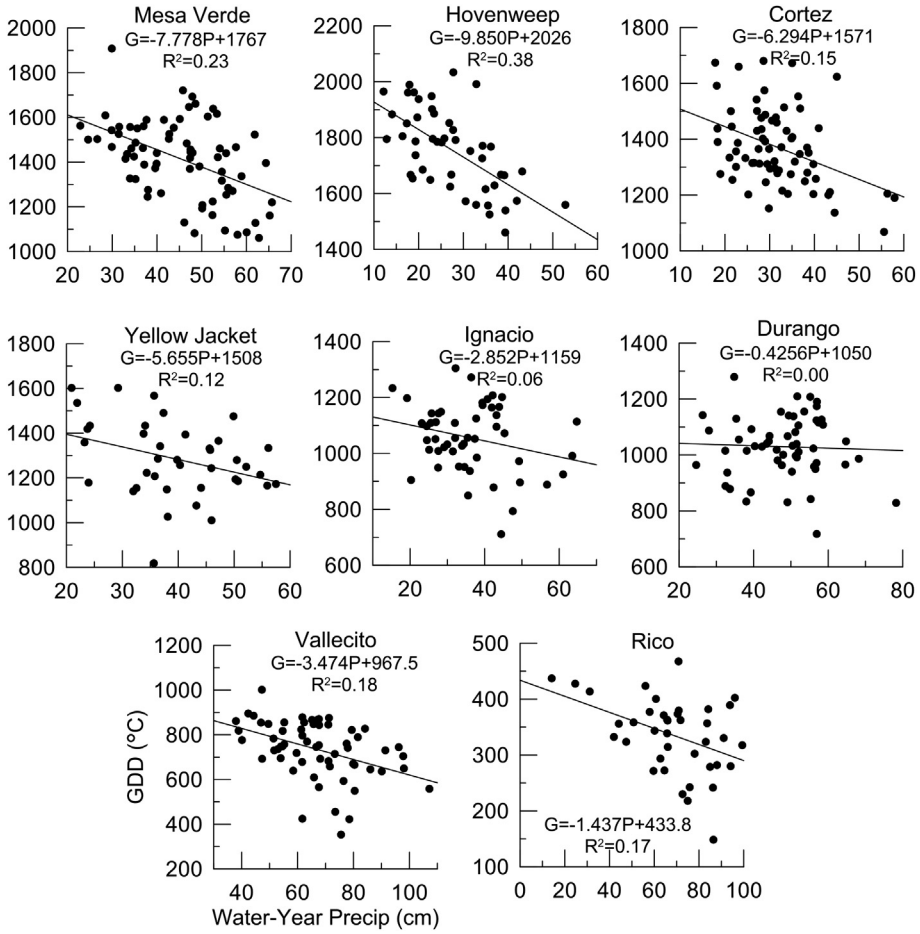

Fig. 10. Growing degree days (GDD) plotted as a function of water-year precipitation. Data from eight weather stations in southwestern Colorado. Note that as it gets wetter at a particular station, it generally gets cooler.

2.8.5. Soil density

In the calculation of a soil's org-N concentration, a soil density of 1.5 g/cm^3 was used. In fact, soil density varies widely with soil type and soil depth; e.g., 133 samples taken from Montezuma county soils have densities ranging from 0.34 to 2.18 g/cm^3 with mean and 1σ values of 1.54 and 0.24 g/cm^3 (National Resources Conservation Service, 2012). Such data could be used to better approximate the range of soil densities associated with each of the seven productive soil groups (Table 2; Supplementary Table 3).

2.8.6. NO_3^- loss from the root volume

In the calculation of org-N mineralization, it was assumed that all NO_3^- produced in the root frustum was available to the maize's root system. This is probably not the case as NO_3^- is highly mobile and can be flushed out of the root zone by infiltrating precipitation. If we assume that the soil is at or below its field capacity at the time of planting, then the NO_3^- produced during the mineralization

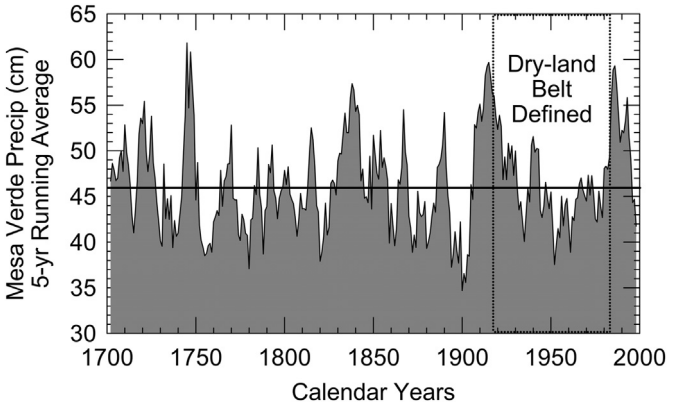

Fig. 11. A five-year running average of reconstructed Mesa Verde precipitation between A.D 1700 and 2000. The rectangle bounded by a dotted line is the time period (1919–1982) over which the dry-land farming belt was defined. This was a generally dry period.

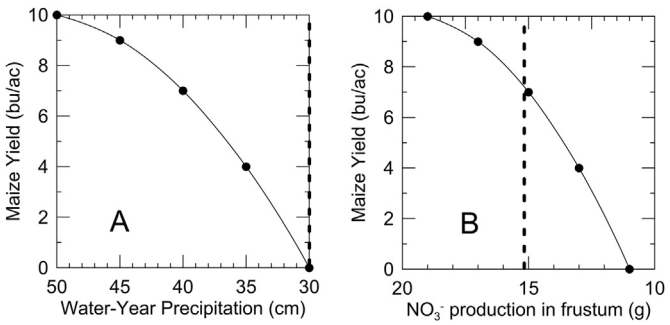

Fig. 12. Hypothetical maize yields as a function of A. water-year precipitation and B. Nitrate production in the root zone frustum. Vertical lines indicate limiting values for maize production.

process will be confined to capillary soil water and will thus be available to the root system. However, if a summer storm should cause the rapid infiltration of rain water, then the NO_3^- captured by the infiltrating water will advect through the soil column and may pass below the root system. Arbuscular mycorrhizal fungi can greatly increase the absorbing surface area of the root. The fungal hyphae can increase the effective volume of the root frustum in that the hyphae can extend between 3 and 7 cm beyond the nitrogen depletion zone that normally develops within the root frustum (Rakshit and Bhadoria, 2008).

This process is exacerbated by the fact that the root system takes about four weeks to reach its maximum depth (see Section 2.4); thus, early summer rains may remove NO_3^- from the deeper parts of the mature root frustum before the roots reach such depths. To model this process, one needs to know if the soil is at or below its field capacity in the early spring and also the frequency, duration and intensity of summer rains. Because winter precipitation is often highly correlated with the ring width of trees such as Douglas fir, the calculation of field capacity is doable; however, there are no proxies for summer precipitation let alone the frequency, duration and intensity of summer precipitation. Therefore, the parameterization of NO_3^- residence time in the root zone would probably have to be done in a somewhat arbitrary manner. Experiments involving the emplacement of lysimeters in the soil zone could be used to understand the flux of water and NO_3^- from the soil zone over the annual cycle, thus enabling calculations of the efficiency of root absorption of NO_3^-.

2.8.7. Scaling of org-N mineralization rate with water-year precipitation

Previously we assigned a 2.0%/yr org-N mineralization rate to a 70-cm water year and a 0.0%/yr mineralization rate to a 0-cm water year. Given that most of the data on org-N and org-C mineralization rates indicate values <1%/yr (Table 4) and that most of the values were obtained from relative wet and humid regions, a mineralization rate of 1%/yr for a 70-cm precipitation rate may be more appropriate. Again, field experiments in which the amount of org-N and NO_3^- in the soil and the flux of NO_3^- from the soil are measured after the field is cleared and not planted would allow calculation of org-N mineralization rates for southwestern Colorado soils.

3. Summary and conclusions

We have presented a relatively simple method for the calculation of prehistoric water-year precipitation throughout the southwestern Colorado study area as a function of time and elevation. Prehistoric water-year precipitation values for Mesa Verde together with a modern-day elevation-dependent precipitation function allowed us to determine the approximate elevations of southwest Colorado precipitation contours for each year since A.D. 480, including the 30-cm contour, which represents the minimum amount of precipitation necessary for the production of maize and the 50-cm contour, which represents the optimum amount of precipitation necessary for the production of maize.

We found that the Great Sage Plain (elevation 1500–2100 m) would have produced some maize during 89% of the time between A.D. 600 and 1350. However, the mid-12th century megadrought was particularly intense, containing several years in which maize would have had to be grown above 2200 m, an elevation associated with a very short growing season. The plot of the 50-cm water-year contour indicates that during only 33% of the time could an optimum crop of maize been produced within the elevation range of the Great Sage Plain and that 23% of the time the 50-cm contour lay above the upper elevation range (2380 m) of the modern dry-land farming belt. We also found that more than 50% of the time, the elevation of the 30-cm precipitation contour would have shifted more than 231 m either up or down within a single year. This suggests that prehistoric Native Americans would have had to generally farm at upper elevations where agriculture was mostly limited by the length and intensity of the summer growing season and (or) they would have had to scatter their fields over a range in elevations in response to the variability in interannual precipitation. If space permitted, the former strategy would have been preferable.

We also presented simple approaches to calculations of maize yield and field life as a function of precipitation and soil group, wherein each soil group is associated with a previously measured org-N distribution. In the future, as human population data become available as a function of space and time, one test of the model would be to plot the elevation and locations of prehistoric Native American villages over time and compare that plot with plots of the 30- and 50-cm water-year precipitation contours with time.

We believe the model of maize productivity presented in this paper represents a substantial improvement relative to the existing VEP maize productivity approach and we look forward to its future testing and improvement.

Acknowledgments

Much of this research was supported by the National Science Foundation under grant DEB-0816400 (Benson) and NOAA grant number NA08OAR4310727 (Stahle). This work supports the Village Ecodynamics Project (VEP) whose objectives include agent-based modeling of the interactions between prehistoric Native Americans who occupied the Four Corners region of the American Southwest, the landscape they occupied, and the climate that impacted the region during the late-thirteenth century. The authors thank Matthew Salzer for access to tree-ring-width data from San Francisco Peaks Bristlecone Pines and to Connie Woodhouse and Jeffrey Lukas for access to updated tree-ring-width data from the Almagre Mountain Bristlecone Pines. The Almagre Mountain C chronology was compiled by Craig Brunstein, using his new collection through 1994, plus D. Graybill's collection through 1983, and V. LaMarche's original chronology through 1968. Daniel Griffin was instrumental in measuring the Douglas fir ring widths and Dorian J. Burnette contributed to the statistical analyses. Stefani Crabtree created Supplementary Fig. 1. Jim Ashby, formerly with the Western Regional Climate Center, went beyond the call of duty to create the historical FFD data sets for the eight weather stations. Timothy Kohler reviewed earlier versions of this manuscript and made a number of excellent suggestions regarding its improvement. Eleanor Griffin was responsible for many of the soil elevation calculations. Thanks also to three anonymous reviewers and William Lipe for their suggestions on how the manuscript could be improved.

Appendix A. Supplementary data

Supplementary data related to this article can be found at http://dx.doi.org/10.1016/j.jas.2013.03.013.

References

Anderson, R.S., 1993. A 35,000 year vegetation and climate history from Potato Lake, Mogollon Rim, Arizona. Quaternary Research 40, 351–359.
Ayers, R.S., 1977. Quality of water for irrigation. Journal of Irrigation and Drainage Division 103, 135–154.
Barron, J.A., Heusser, L., Herbert, T., Lyle, M., 2003. High-resolution climatic evolution of coastal northern California during the past 16,000 years. Paleoceanography 18, 1020. http://dx.doi.org/10.1029/2002PA000768.
Bellorado, B.A., 2007. Breaking Down the Models: Reconstruction Prehistoric Subsistence Agriculture in the Durango District of Southwestern Colorado. M.A. dissertation. Northern Arizona University, Flagstaff.

Benson, L.V., Berry, M.S., 2009. Climate change and cultural response in the prehistoric American Southwest. Kiva 75, 89–119.
Benson, L.V., 2010a. Factors controlling pre-Columbian and early historic maize productivity in the American southwest, Part 2: the Chaco Halo, Mesa Verde, Pajarito Plateau/Bandelier, and Zuni archaeological regions. Journal of Archaeological Method and Theory 18, 61–109.
Benson, L.V., 2010b. Factors controlling pre-Columbian and early historic maize productivity in the American southwest, Part 1: the southern Colorado Plateau and Rio Grande regions. Journal of Archaeological Method and Theory 18, 1–60.
Bradfield, M., 1971. The Changing Pattern of Hopi Agriculture. Royal Anthropological Institute. Occasional Paper No. 30.
Briffa, K.R., Osborn, T.J., Schweingruber, F.H., Farris, I.C., Jones, P.D., Shiyatov, S.G., Vaganov, E.A., 2001. Low-frequency temperature variations from a northern tree ring density network. Journal of Geophysical Research 106, 2929–2941.
Burns, B.T., 1983. Simulated Anasazi Storage Behavior Using Crop Yields Reconstructed from Tree Rings. Ph.D. dissertation. University of Arizona, Tucson.
Clay, D.E., Clapp, C.E., Reese, C., Liu, Z., Carlson, C.G., Woodward, H., Bly, A., 2007. Carbon-13 fractionation of relic soil organic carbon during mineralization effects calculated half-lives. Soil Science Society of America Journal 71, 1003–1009.
Dix, R.L., Richards, J.L., 1976. Possible change in spectra structure of the subalpine forest induced by increased snowpack. In: Steinhoff, H.W., Ives, J.D. (Eds.), Ecological Impacts of Snowpack Augmentation in the San Juan Mountains, Colorado. Ecology Project Final Report, Colorado State University, Fort Collins, pp. 311–322.
Doran, J.W., Elliot, E.T., Paustian, K., 1998. Soil microbial activity, nitrogen cycling, and long-term changes in organic carbon pools as related to fallow tillage management. Soil Tillage Research 49, 3–18.
Dwyer, L.M., Ma, B.L., Stewart, D.W., Hayhoe, H.N., Bachin, D., Culley, J.L.B., McGovern, M., 1996. Root mass distribution under conventional and conservation tillage. Canadian Journal of Soil Science 76, 23–28.
Fehrenbacher, J.B., Rust, R.H., 1956. Corn root penetration in soils derived from various textures of Wisconsin-age glacial till. Soil Science 82, 369–378.
Griffin, D., Meko, D.M., Touchan, R., Leavitt, S.W., Woodhouse, C.A., 2011. Latewood chronology development for summer-moisture reconstruction in the US Southwest. Tree-ring Research 67, 87–101.
Hanway, D.G., 1966. Irrigation. In: Pierre, W.H. (Ed.), Advances in Corn Production: Principles and Practices. Iowa State University Press, Ames, pp. 155–176.
Herrmann, A., 2003. Predicting Nitrogen Mineralization from Soil Organic Matter – a Chimera?. Ph.D. dissertation Swedish University of Agricultural Sciences, Uppsala.
Hoeft, R.G., Peck, T.R., 2002. Soil testing and fertility. In: Hoeft, R.G., Nafziger, E. (Eds.), The Illinois Agronomy Handbook. University of Illinois Extension, Urbana-Champaign, pp. 91–131.
Holmes, T., Crow, W., Jackson, T., 2011. Development of a Continuous Multi-satellite Land Surface Temperature Product. U.S. Department of Agriculture. Beltsville Agricultural Research Center Poster Day, Abstract 15.
Jenkins, M.T., 1941. Influence of climate and weather on growth of corn. In: Hambidge, G. (Ed.), Climate and Man, Yearbook of Agriculture, 1941. U.S. Department of Agriculture, Washington, D.C., pp. 308–341.
Jenkinson, D.S., Rayner, J.H., 1977. The turnover of soil organic matter in some of the Rothamsted classical experiments. Soil Science 123, 298–305.
Kohler, T.A., 2012. Modeling agricultural productivity and farming effort. In: Kohler, T.A., Varien, M.D. (Eds.), Emergence and Collapse of Early Villages, Models of Central Mesa Verde Archaeology. University of California Press, Berkeley, pp. 85–112.
Kohler, T.A., Bocinsky, R.K., Cockburn, D., Crabtree, S.A., Varien, M.D., Kolm, K.E., Smith, S., Ortman, S.G., Kobti, Z., 2012. Modelling prehispanic Pueblo societies in their ecosystems. Ecological Modelling 241, 30–41.
Leavitt, S.W., Woodhouse, C.A., Castro, C.L., Wright, W.E., Meko, D.M., Touchan, R., Griffin, D., Ciancarelli, B., 2011. The North American monsoon in the US Southwest: potential for investigation with tree-ring carbon isotopes. Quaternary International 235, 101–107.
Leonard, W.H., Brandon, J.F., Curtis, J.J., 1940. Corn Production in Colorado. In: Colorado Experiment Station Bulletin 463. Fort Collins.
Meko, D.M., Baisan, C.H., 2001. Pilot study of latewood-width of conifers as an indicator of variability of summer rainfall in the North American Monsoon region. International Journal of Climatology 21, 697–708.
Muenchrath, D.A., Kuratomi, M., Sandor, J.A., Homburg, J.A., 2002. Observational study of maize production in semiarid New Mexico. Journal of Ethnobiology 22, 1–33.
National Resources Conservation Service, 2012. http://soils.usda.gov/.
Nielson, R.L., 2012. Drought and Heat Stress Effects on Corn Pollination. http://www.agry.purdue.edu/ext/corn/news/articles.96/p&c9635.htm (accessed 12.07.12.).
Petersen, K.L., 1987a. Tree-ring transfer functions for estimating corn production. In: Petersen, K.L., Orcutt, J.D. (Eds.), Dolores Archaeological Program: Supporting Studies: Settlement and Environment. United States Department of the Interior, Bureau of Reclamation Engineering and Research Center, Denver, pp. 217–231.
Petersen, K.L., 1987b. Reconstruction of droughts for the Dolores project area using tree-ring studies. In: Petersen, K.L., Orcutt, J.D. (Eds.), Dolores Archaeological Program: Supporting Studies: Settlement and Environment. United States Department of the Interior, Bureau of Reclamation Engineering and Research Center, Denver, pp. 91–102.
Petersen, K.L., 1988. Climate and the Dolores River Anasazi. University of Utah. Anthropological Papers No. 113.
Petersen, K.L., 1994. A warm and wet little climatic optimum and a cold and dry Little Ice Age in the southern Rocky Mountains, U.S.A. Climatic Change 26, 243–269.
Petersen, K.L., Mehringer Jr., P.J., 1976. Postglacial timberline fluctuations, LaPlata Mountains, southwestern Colorado. Arctic and Alpine Research 8, 275–288.
Qin, R., Stamp, P., Richner, W., 2006. Impact of tillage on maize rooting in a Cambisol and Luvisol in Switzerland. Soil & Tillage Research 85, 50–61.
Rakshit, A., Bhadoria, P., 2008. Measurement of arbuscular mycorrhizal hyphal length and prediction of P influx by mechanistic model. World Journal of Agricultural Sciences 4, 23–27.
Ramsey, D.K., 1997. Soil Survey of Cortez Area, Colorado, Parts of Dolores and Montezuma Counties. United States Department of Agriculture, Natural Resources Conservation Service.
Salzer, M.W., Kipfmueller, K.F., 2005. Reconstructed temperature and precipitation on a millennial timescale from tree-rings in the southern Colorado Plateau, U.S.A. Climatic Change 70, 465–487.
Shaw, R.H., 1988. Climate requirement. In: Sprague, G.F., Dudley, J.W. (Eds.), Corn and Corn Improvement, third ed. American Society of Agronomy, Madison, pp. 609–638.
Soudi, B., Sbai, A., Chiang, C.N., 1990. Nitrogen mineralization in semiarid soils of Morocco: rate constant variation with depth. Soil Science Society of America Journal 54, 756–761.
Theroux, S., D'Andrea, W.J., Toney, J., Amaral-Zettleer, L., Huang, Y., 2010. Phylogenetic diversity and evolutionary relatedness of alkenones-producing haptophyte algae in lakes: implications for continental paleotemperature reconstructions. Earth and Planetary Science Letters 300, 311–320.
Thomison, P., Lipps, P., Hammond, R., Mullen, R., Eisley, B., 2012. Ohio Agronomy Guide, fourteenth ed.. Bulletin 472–05. http://ohioline.osu.edu/b472/0005.html (accessed 13.07.12.).
Van West, C.R., 1994. Modeling Prehistoric Climatic Variability and Agricultural Production in Southwestern Colorado: a GIS Approach. In: Reports of Investigations 67. Washington State University Department of Anthropology, Pullman.
Weaver, J.E., 1926. Root Development of Field Crops. McGraw-Hill Book Company, London.
Western Regional Climate Center. http://www.wrcc.dri.edu/, last accessed July 2012.
Williams, M.A., Rice, C.W., Owensby, C.E., 2000. Carbon dynamics and microbial activity in tallgrass prairie exposed to elevated CO_2 for 8 years. Plant Soil 227, 127–137.
Wright, A.M., 2012. Low-frequency climate in the Mesa Verde region. In: Kohler, T.A., Varien, M.D. (Eds.), Emergence and Collapse of Early Villages, Models of Central Mesa Verde Archaeology. University of California Press, Berkeley, pp. 41–57.

Further readings

Dean, J.S., Robinson, W.S., 1978. Expanded Tree-ring Chronologies for the Southwestern United States. In: Chronology Series, vol. 3. Laboratory of Tree-Ring Research, University of Arizona, Tucson.
Honeycutt, L., 1995. Dryland gardening in southwest Colorado: past and present. In: Toll, H.W. (Ed.), Soil, Water, Biology, and Belief in Prehistoric and Traditional Southwestern Agriculture. New Mexico Archaeological Council Special Publication, No. 2, Albuquerque, pp. 369–373.
World Data Center for Paleoclimatology, 2003. http://hurrican.ncdc.noaa.gov/pls/paleo (accessed 03.03.03.).

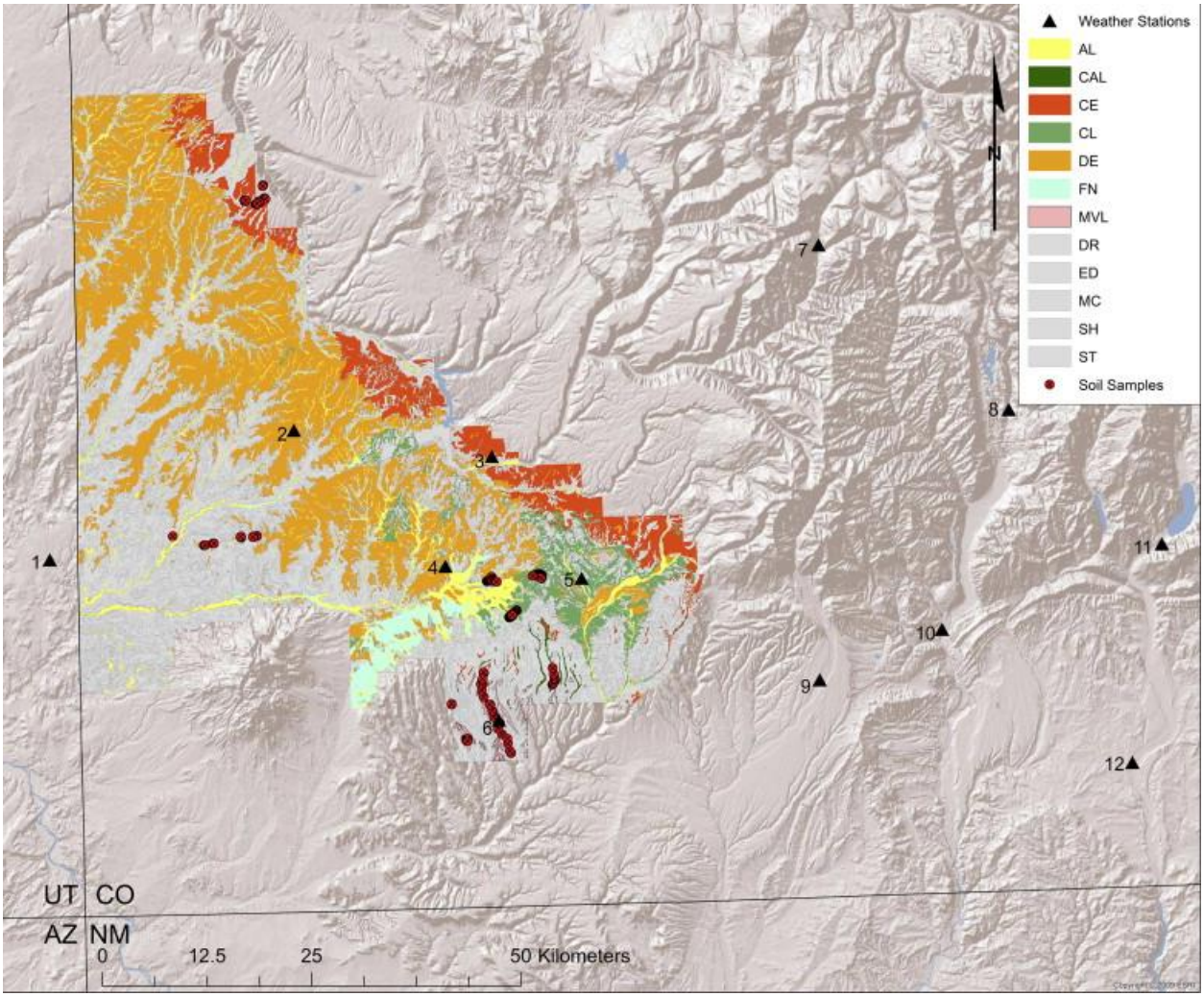

Supplementary Fig. S1.

Distribution of seven soil groups suitable for farming and five soil groups that unsuitable for farming in southwestern Colorado. Soil sampling sites are shown as red dots; weather station sites are shown as black triangles.

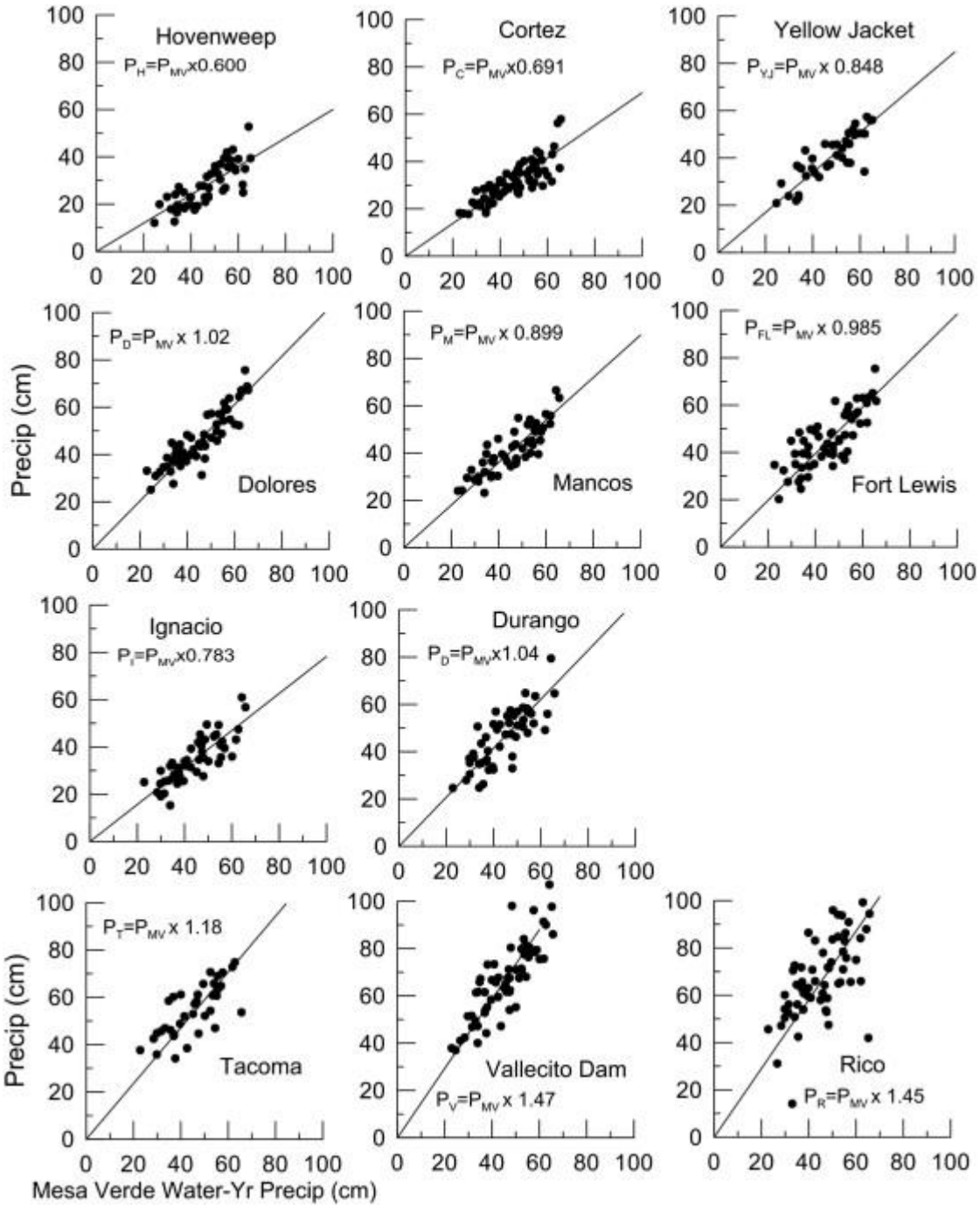

Supplementary Fig. S2.

Correlations of Mesa Verde water-year precipitation with water-year precipitation from 11 weather stations in southwestern Colorado. All regressions have been forced to pass through $x = 0$, $y = 0$.

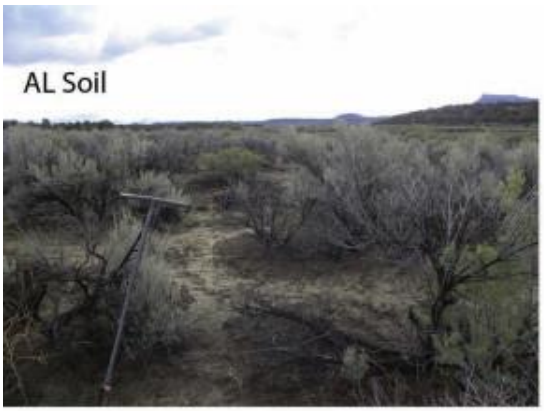
AL Soil


CAL Soil


CL Soil


DE Soil


FN Soil


MVL Soil


CE Soil

Supplementary Fig. 3.

Vegetation covering seven southwestern Colorado soil groups suitable for prehistoric agriculture. AL, CAL, CL, DE, FN, MVL, and CE stand, respectively for alluvial, Mesa Verde alluvial, clay, deep eolian, alluvial fan, Mesa Verde eolian, and cool eolian soils.

Supplementary Table 1. Reconstructed water-year precipitation for Mesa Verde

	precipitation (cm)									
Year (AD)	1	2	3	4	5	6	7	8	9	10
60	39.4	36.3	37.4	39.5	64.1	43.1	43.7	73.2	34.3	42.4
61	24.9	54.8	38.5	37.3	37.7	40.5	47.3	59.7	41.7	19.9
62	87.4	51.9	52.5	53.4	41.6	41.8	50.7	51.0	49.3	42.6
63	51.9	39.9	32.6	32.3	47.0	74.4	42.1	47.1	33.1	41.0
64	43.9	47.7	39.0	37.9	32.3	34.4	42.9	43.7	54.1	36.9
65	43.1	43.6	43.8	45.2	44.5	51.0	46.4	45.1	52.6	32.8
66	37.4	47.1	32.6	33.8	48.3	51.5	51.4	50.4	48.4	56.5
67	43.3	62.9	56.4	66.8	59.7	56.3	48.3	45.9	54.6	53.6
68	49.8	57.5	54.5	48.6	57.1	43.9	56.5	51.9	61.7	54.5
69	69.1	43.8	65.5	54.2	61.2	56.6	37.1	64.6	50.7	58.9
70	50.7	47.3	43.0	25.6	45.1	23.2	26.3	42.0	29.4	47.6
71	41.0	44.8	47.0	43.1	46.7	39.5	22.6	40.9	51.5	54.8
72	36.4	44.2	42.2	24.5	66.0	53.2	55.9	49.9	50.9	61.2
73	54.5	51.5	65.9	32.9	52.3	51.6	59.3	13.9	46.4	49.2
74	46.8	30.7	54.2	49.2	39.8	49.2	54.1	38.2	53.1	38.3
75	21.3	45.0	50.6	40.2	46.3	43.5	36.0	58.0	52.2	41.0
76	57.8	47.2	44.9	40.4	63.1	51.0	37.0	54.0	46.6	34.1
77	42.3	55.3	44.3	27.5	43.4	48.4	46.1	17.7	31.1	57.4
78	46.5	51.0	47.2	60.4	55.6	40.8	66.1	34.5	54.9	55.5
79	50.8	50.2	53.0	62.9	27.5	65.7	23.8	58.4	48.8	58.2
80	32.7	71.2	67.2	53.6	52.3	46.4	49.2	35.1	20.3	68.3
81	42.6	40.9	43.7	60.4	51.6	45.6	34.5	49.4	29.9	60.5
82	63.5	55.7	26.1	55.1	37.2	53.3	35.4	61.2	26.6	34.0
83	48.3	55.4	48.2	40.2	34.3	52.6	38.1	55.6	40.9	28.8
84	46.1	33.4	56.5	34.3	55.6	46.2	25.7	57.2	44.3	49.4
85	39.7	67.3	52.7	62.1	50.3	61.5	27.6	59.1	32.5	53.7
86	50.6	63.0	25.1	63.4	49.4	40.1	30.6	39.0	66.6	36.1
87	55.7	43.5	51.4	45.6	46.1	59.6	28.8	35.8	47.8	31.9
88	50.7	42.7	34.3	27.6	49.6	44.8	47.5	47.0	48.4	57.0
89	42.8	33.2	52.0	30.1	34.8	67.1	53.6	51.1	72.8	58.3
90	26.7	59.9	32.7	39.2	55.3	20.4	27.1	52.3	53.3	54.2
91	62.8	57.5	55.5	59.0	50.5	40.1	57.2	49.5	58.0	41.1
92	54.6	28.6	28.5	32.7	44.5	46.5	40.1	49.9	55.3	31.1
93	51.2	45.9	42.6	46.7	45.4	47.4	31.2	50.6	34.0	42.8
94	49.6	48.8	44.1	48.5	47.8	56.6	53.7	56.9	53.0	52.1
95	42.1	58.3	32.7	36.8	33.5	62.5	28.1	36.7	45.5	59.7
96	37.8	60.4	47.6	51.6	34.4	66.5	48.9	40.8	36.1	50.1
97	54.1	20.5	81.5	62.0	36.1	42.7	63.0	34.1	46.1	19.5
98	26.8	56.3	29.4	38.5	49.3	45.2	72.7	73.7	80.6	46.0
99	25.3	48.9	41.0	48.3	45.3	54.1	42.8	49.0	42.0	49.8
100	34.0	36.1	49.2	43.7	20.5	58.9	56.4	55.8	25.2	46.4
101	49.0	47.0	36.1	48.5	56.2	52.1	59.2	35.9	24.0	60.3
102	51.4	46.2	52.4	58.7	55.1	46.3	50.7	49.6	48.2	31.2
103	46.8	30.9	35.2	50.1	28.9	35.0	53.6	38.6	44.9	45.7
104	29.3	55.6	40.6	34.3	43.6	30.3	52.4	30.7	55.8	48.3
105	38.6	54.9	39.0	53.8	29.8	58.0	45.4	55.5	47.7	44.5
106	54.8	29.3	81.6	66.3	76.2	50.6	34.2	32.3	51.6	46.5
107	33.5	47.8	45.2	45.2	51.6	51.1	51.1	46.7	56.0	71.1
108	33.2	42.6	41.5	53.9	24.4	44.1	57.3	53.3	49.1	21.9
109	37.2	49.6	31.1	41.7	42.5	44.7	36.7	41.3	31.1	47.5

110	33.4	60.6	47.3	40.4	52.3	33.9	49.1	41.0	43.9	50.1
111	45.8	63.8	42.4	57.3	55.0	67.7	71.9	55.6	60.9	48.5
112	39.4	69.7	29.8	64.1	43.3	27.4	53.4	50.9	56.0	39.4
113	32.3	50.6	36.8	50.1	41.4	43.1	39.9	46.6	42.2	31.8
114	46.9	42.1	41.1	44.0	51.0	32.8	39.6	43.0	46.5	23.2
115	33.2	66.2	49.8	35.2	56.8	23.4	51.7	27.4	68.8	45.9
116	25.9	60.4	58.6	36.0	50.3	24.0	59.2	31.3	29.9	45.4
117	43.9	37.9	39.2	34.9	29.9	44.3	33.1	53.7	25.9	50.1
118	52.3	26.1	44.5	61.9	46.5	23.8	48.6	46.2	52.7	57.5
119	25.6	44.3	55.0	52.3	60.1	56.0	67.8	39.3	39.2	81.5
120	51.7	29.8	56.3	48.5	29.9	54.1	41.7	44.9	68.3	58.0
121	43.7	39.4	44.2	38.2	30.2	32.5	30.6	40.1	55.1	51.8
122	41.0	43.6	63.6	38.3	49.4	47.8	22.0	41.8	56.1	41.8
123	35.4	38.4	53.7	35.9	36.4	32.7	38.2	47.8	41.8	30.8
124	43.9	44.4	46.2	42.6	47.2	38.2	49.2	63.7	54.7	45.1
125	41.5	47.7	57.4	20.1	53.2	49.5	50.8	36.8	49.8	44.0
126	53.3	58.0	30.5	54.1	51.6	43.6	49.2	48.3	62.7	44.5
127	72.2	52.2	28.3	36.9	46.9	32.6	39.5	30.9	42.6	30.1
128	45.9	43.7	29.1	42.0	36.4	45.7	40.9	33.9	49.5	57.3
129	46.9	36.3	47.3	48.7	24.3	45.3	42.1	52.5	35.7	45.3

Supplementary Table 2. Grouping of soil units by code and unit number

Unit	Map Unit Name	Map Unit Type	Code
1	Ackmen loam, 1 to 3 percent slopes	Consociation	AL
2	Ackmen loam, 3 to 6 percent slopes	Consociation	AL
3	Arabrab loamy sand, 3 to 9 percent slopes	Consociation	SH
4	Arabrab-Longburn complex, 3 to 15 percent slopes	Complex	SH
5	Archuleta-Sanchez complex, 12 to 65 percent slopes	Complex	ST
6	Argiustolls-Haplustalfs complex, 30 to 80 percent slopes	Complex	ST
7	Argiustolls-Haplustalfs-Rock outcrop complex, 30 to 80 percent slopes	Complex	ST
8	Barx loam, 3 to 6 percent slopes	Consociation	DE
9	Barx loam, 6 to 12 percent slopes	Consociation	DE
10	Barx very fine sandy loam, 1 to 4 percent slopes	Consociation	DE
11	Barx-Gapmesa complex, 2 to 6 percent slopes	Complex	DE
12	Battlerock clay loam, 0 to 6 percent slopes	Consociation	AL
13	Beje-Tragmon complex, 3 to 9 percent slopes	Complex	CE
14	Burnson loam, 1 to 15 percent slopes	Consociation	CE
15	Burnson loam, dry, 1 to 15 percent slopes	Consociation	CE
16	Burnson-Herm complex, 15 to 30 percent slopes	Complex	CE
17	Cahona loam, 1 to 3 percent slopes	Consociation	DE
18	Cahona loam, 3 to 6 percent slopes	Consociation	DE
19	Cahona loam, 6 to 12 percent slopes	Consociation	DE
20	Cahona-Pulpit complex, 3 to 9 percent slopes	Complex	DE
21	Cahona-Sharps-Wetherill complex, 2 to 6 percent slopes	Complex	DE
22	Claysprings very stony clay loam, 12 to 65 percent slopes	Consociation	DR
23	Collide clay loam, 3 to 6 percent slopes	Consociation	DE
24	Collide clay loam, 6 to 12 percent slopes	Consociation	DE
25	Collide complex, 0 to 2 percent slopes	Complex	DE
26	Collide complex, 2 to 6 percent slopes	Complex	DE
27	Dalmatian-Apmay-Schrader complex, 0 to 5 percent slopes	Complex	AL
28	Dam	Consociation	MC
29	Endoaquolls-Ustifluvents complex, 0 to 5 percent slopes	Complex	AL
30	Falconry gravelly fine sandy loam, 3 to 25 percent slopes	Consociation	SH
31	Farb-Rock outcrop complex, 3 to 12 percent slopes	Complex	SH
32	Fardraw loam, 3 to 15 percent slopes	Consociation	CE
33	Fardraw very cobbly loam, 0 to 9 percent slopes	Consociation	CE
34	Fardraw very cobbly loam, 9 to 25 percent slopes	Consociation	CE
35	Fardraw-Granath complex, 3 to 12 percent slopes	Complex	CE
36	Fivepine-Nortez complex, 0 to 15 percent slopes	Complex	CE
37	Fluvaquents-Haplustolls complex, 0 to 5 percent slopes	Complex	AL
38	Fluvents-Fluvaquents complex, 0 to 3 percent slopes	Complex	AL
39	Fughes loam, 1 to 12 percent slopes	Consociation	CE
40	Fughes-Herm complex, 5 to 25 percent slopes	Complex	CE

Unit	Map Unit Name	Map Unit Type	Code
1	Ackmen loam, 1 to 3 percent slopes	Consociation	AL
2	Ackmen loam, 3 to 6 percent slopes	Consociation	AL
27	Dalmatian-Apmay-Schrader complex, 0 to 5 percent slopes	Complex	AL
29	Endoaquolls-Ustifluvents complex, 0 to 5 percent slopes	Complex	AL
37	Fluvaquents-Haplustolls complex, 0 to 5 percent slopes	Complex	AL
12	Battlerock clay loam, 0 to 6 percent slopes	Consociation	AL
38	Fluvents-Fluvaquents complex, 0 to 3 percent slopes	Complex	AL
62	Irak loam, 0 to 3 percent slopes	Consociation	AL
65	Lillings silt loam, sodic, 1 to 3 percent slopes	Consociation	AL
66	Lillings silty clay loam, 1 to 3 percent slopes	Consociation	AL
67	Lillings silty clay loam, 3 to 6 percent slopes	Consociation	AL
84	Payter sandy loam, 3 to 15 percent slopes	Consociation	AL
88	Pogo loam, 0 to 2 percent slopes	Consociation	AL
96	Purcella loam, 0 to 3 percent slopes	Consociation	AL
97	Ramper clay loam, 0 to 3 percent slopes	Consociation	AL
98	Ramper loam, 0 to 3 percent slopes	Consociation	AL
99	Ravola clay loam, 0 to 3 percent slopes	Consociation	AL
134	Umbarg-Winner-Tesajo complex, 0 to 2 percent slopes	Complex	AL
136	Ustic Torriorthents-Gullied land complex, 1 to 60 percent slopes	Complex	AL
55	Hesperus sandy loam, 3 to 12 percent slopes	Consociation	CAL
132	Typic Argiaquolls, 0 to 3 percent slopes	Consociation	CAL
13	Beje-Tragmon complex, 3 to 9 percent slopes	Complex	CE
14	Burnson loam, 1 to 15 percent slopes	Consociation	CE
15	Burnson loam, dry, 1 to 15 percent slopes	Consociation	CE
16	Burnson-Herm complex, 15 to 30 percent slopes	Complex	CE
32	Fardraw loam, 3 to 15 percent slopes	Consociation	CE
33	Fardraw very cobbly loam, 0 to 9 percent slopes	Consociation	CE
34	Fardraw very cobbly loam, 9 to 25 percent slopes	Consociation	CE
35	Fardraw-Granath complex, 3 to 12 percent slopes	Complex	CE
36	Fivepine-Nortez complex, 0 to 15 percent slopes	Complex	CE
39	Fughes loam, 1 to 12 percent slopes	Consociation	CE
40	Fughes-Herm complex, 5 to 25 percent slopes	Complex	CE
41	Fughes-Sheek complex, 15 to 30 percent slopes	Complex	CE
43	Goldbug very stony fine sandy loam, 5 to 30 percent slopes	Consociation	CE
44	Granath loam, 3 to 6 percent slopes	Consociation	CE
45	Granath loam, 6 to 12 percent slopes	Consociation	CE
46	Granath-Fughes complex, 0 to 15 percent slopes	Complex	CE
47	Granath-Nortez complex, 0 to 15 percent slopes	Complex	CE
48	Granath-Ormiston-Fivepine complex, 0 to 15 percent slopes	Complex	CE
49	Herm loam, 6 to 25 percent slopes	Consociation	CE

41	Fughes-Sheek complex, 15 to 30 percent slopes	Complex	CE	50	Herm very cobbly loam, 15 to 40 percent slopes	Consociation	CE
42	Gladel-Pulpit complex, 3 to 9 percent slopes	Complex	SH	51	Herm-Pagoda complex, 0 to 15 percent slopes	Complex	CE
43	Goldbug very stony fine sandy loam, 5 to 30 percent slopes	Consociation	CE	52	Hesperus loam, 0 to 3 percent slopes	Consociation	CE
44	Granath loam, 3 to 6 percent slopes	Consociation	CE	53	Hesperus loam, 3 to 6 percent slopes	Consociation	CE
45	Granath loam, 6 to 12 percent slopes	Consociation	CE	54	Hesperus loam, 6 to 12 percent slopes	Consociation	CE
46	Granath-Fughes complex, 0 to 15 percent slopes	Complex	CE	56	Ilex loam, 3 to 12 percent slopes	Consociation	CE
47	Granath-Nortez complex, 0 to 15 percent slopes	Complex	CE	57	Ilex loam, 12 to 25 percent slopes	Consociation	CE
48	Granath-Ormiston-Fivepine complex, 0 to 15 percent slopes	Complex	CE	58	Ilex-Granath complex, 2 to 6 percent slopes	Complex	CE
49	Herm loam, 6 to 25 percent slopes	Consociation	CE	59	Ilex-Granath complex, 6 to 12 percent slopes	Complex	CE
50	Herm very cobbly loam, 15 to 40 percent slopes	Consociation	CE	60	Ilex-Pramiss-Falconry complex, 3 to 20 percent slopes	Complex	CE
51	Herm-Pagoda complex, 0 to 15 percent slopes	Complex	CE	61	Ilex-Pramiss-Granath complex, 2 to 9 percent slopes	Complex	CE
52	Hesperus loam, 0 to 3 percent slopes	Consociation	CE	63	Jemco-Detra-Beje complex, 1 to 15 percent slopes	Complex	CE
53	Hesperus loam, 3 to 6 percent slopes	Consociation	CE	81	Ormiston-Fivepine complex, 0 to 15 percent slopes	Complex	CE
54	Hesperus loam, 6 to 12 percent slopes	Consociation	CE	82	Ormiston-Granath complex, 1 to 12 percent slopes	Complex	CE
55	Hesperus sandy loam, 3 to 12 percent slopes	Consociation	CAL	83	Ormiston-Nortez complex, 3 to 12 percent slopes	Complex	CE
56	Ilex loam, 3 to 12 percent slopes	Consociation	CE	90	Pramiss-Granath complex, 3 to 9 percent slopes	Complex	CE
57	Ilex loam, 12 to 25 percent slopes	Consociation	CE	102	Ricot loam, 1 to 3 percent slopes	Consociation	CE
58	Ilex-Granath complex, 2 to 6 percent slopes	Complex	CE	103	Ricot loam, 3 to 6 percent slopes	Consociation	CE
59	Ilex-Granath complex, 6 to 12 percent slopes	Complex	CE	104	Ricot loam, 6 to 12 percent slopes	Consociation	CE
60	Ilex-Pramiss-Falconry complex, 3 to 20 percent slopes	Complex	CE	123	Sideshow silty clay loam, 0 to 3 percent slopes	Consociation	CL
61	Ilex-Pramiss-Granath complex, 2 to 9 percent slopes	Complex	CE	124	Sideshow silty clay loam, 3 to 6 percent slopes	Consociation	CL
62	Irak loam, 0 to 3 percent slopes	Consociation	AL	125	Sideshow silty clay loam, 6 to 12 percent slopes	Consociation	CL
63	Jemco-Detra-Beje complex, 1 to 15 percent slopes	Complex	CE	126	Sideshow-Zigzag complex, 3 to 25 percent slopes	Complex	CL
64	Lazear-Rock outcrop complex, 12 to 65 percent slopes	Complex	SH	127	Sideslide silty clay loam, 3 to 9 percent slopes	Consociation	CL
65	Lillings silt loam, sodic, 1 to 3 percent slopes	Consociation	AL	8	Barx loam, 3 to 6 percent slopes	Consociation	DE
66	Lillings silty clay loam, 1 to 3 percent slopes	Consociation	AL	9	Barx loam, 6 to 12 percent slopes	Consociation	DE
67	Lillings silty clay loam, 3 to 6 percent slopes	Consociation	AL	10	Barx very fine sandy loam, 1 to 4 percent slopes	Consociation	DE
68	Longburn-Rock outcrop complex, 10 to 45 percent slopes	Complex	SH	11	Barx-Gapmesa complex, 2 to 6 percent slopes	Complex	DE
69	Longburn-Rock outcrop complex, 45 to 80 percent slopes	Complex	SH	17	Cahona loam, 1 to 3 percent slopes	Consociation	DE
70	Mack fine sandy loam, 0 to 6 percent slopes	Consociation	ED	18	Cahona loam, 3 to 6 percent slopes	Consociation	DE
71	Mikett clay loam, saline-sodic, 0 to 3 percent slopes	Consociation	FN	19	Cahona loam, 6 to 12 percent slopes	Consociation	DE
72	Mikett clay loam, 0 to 3 percent slopes	Consociation	FN	20	Cahona-Pulpit complex, 3 to 9 percent slopes	Complex	DE
73	Mikim clay loam, 1 to 3 percent slopes	Consociation	FN	21	Cahona-Sharps-Wetherill complex, 2 to 6 percent slopes	Complex	DE
74	Mikim clay loam, sodic, 0 to 3 percent slopes	Consociation	FN	23	Collide clay loam, 3 to 6 percent slopes	Consociation	DE
75	Mikim loam, 3 to 6 percent slopes	Consociation	FN	24	Collide clay loam, 6 to 12 percent slopes	Consociation	DE
76	Morefield loam, 1 to 3 percent slopes	Consociation	MVL	25	Collide complex, 0 to 2 percent slopes	Complex	DE
77	Morefield loam, 3 to 6 percent slopes	Consociation	MVL	26	Collide complex, 2 to 6 percent slopes	Complex	DE
78	Nortez-Granath complex, 0 to 6 percent slopes	Complex	DE	78	Nortez-Granath complex, 0 to 6 percent slopes	Complex	DE
79	Northrim cobbly loam, 15 to 40 percent slopes	Consociation	ST	85	Pinacol loam, 1 to 12 percent slopes	Consociation	DE
80	Ormiston-Beje complex, 5 to 30 percent slopes	Complex	ST	93	Pulpit loam, 3 to 12 percent slopes	Consociation	DE
81	Ormiston-Fivepine complex, 0 to 15 percent slopes	Complex	CE	94	Pulpit loam, 3 to 6 percent slopes	Consociation	DE
82	Ormiston-Granath complex, 1 to 12 percent slopes	Complex	CE	95	Pulpit loam, 6 to 12 percent slopes	Consociation	DE
83	Ormiston-Nortez complex, 3 to 12 percent slopes	Complex	CE	112	Sharps loam, 3 to 6 percent slopes	Consociation	DE

84	Payter sandy loam, 3 to 15 percent slopes	Consociation	AL
85	Pinacol loam, 1 to 12 percent slopes	Consociation	DE
86	Pinacol loam, 12 to 40 percent slopes	Consociation	ST
87	Pits	Consociation	MC
88	Pogo loam, 0 to 2 percent slopes	Consociation	AL
89	Pramiss very cobbly loam, 6 to 25 percent slopes	Consociation	ST
90	Pramiss-Granath complex, 3 to 9 percent slopes	Complex	CE
91	Prater loam, 10 to 25 percent slopes	Consociation	ST
92	Prater-Dolcan complex, 25 to 60 percent slopes	Complex	ST
93	Pulpit loam, 3 to 12 percent slopes	Consociation	DE
94	Pulpit loam, 3 to 6 percent slopes	Consociation	DE
95	Pulpit loam, 6 to 12 percent slopes	Consociation	DE
96	Purcella loam, 0 to 3 percent slopes	Consociation	AL
97	Ramper clay loam, 0 to 3 percent slopes	Consociation	AL
98	Ramper loam, 0 to 3 percent slopes	Consociation	AL
99	Ravola clay loam, 0 to 3 percent slopes	Consociation	AL
100	Recapture fine sandy loam, 0 to 6 percent slopes	Consociation	ED
101	Recapture sandy loam, 0 to 6 percent slopes	Consociation	ED
102	Ricot loam, 1 to 3 percent slopes	Consociation	CE
103	Ricot loam, 3 to 6 percent slopes	Consociation	CE
104	Ricot loam, 6 to 12 percent slopes	Consociation	CE
105	Rizno-Gapmesa complex, 3 to 9 percent slopes	Complex	ED
106	Rizno-Littlenan-Bodry association, 3 to 50 percent slopes	Association	ED
107	Rizno-Ruinpoint-Rock outcrop complex, 1 to 15 percent slopes	Complex	DR
108	Rock outcrop	Consociation	MC
109	Romberg-Crosscan complex, 6 to 25 percent slopes	Complex	ST
110	Romberg-Crosscan-Rock outcrop complex, 25 to 80 percent slopes	Complex	ST
111	Roubideau loam, 1 to 6 percent slopes	Consociation	MVL
112	Sharps loam, 3 to 6 percent slopes	Consociation	DE
113	Sharps loam, 6 to 12 percent slopes	Consociation	DE
114	Sharps loam, dry, 6 to 12 percent slopes	Consociation	DE
115	Sharps, dry-Gapmesa complex, 6 to 12 percent slopes	Complex	DE
116	Sharps-Cahona complex, 6 to 12 percent slopes	Complex	DE
117	Sharps-Pulpit complex, 2 to 6 percent slopes	Complex	DE
118	Sharps-Pulpit complex, 6 to 12 percent slopes	Complex	DE
119	Sheek-Archuleta complex, 6 to 25 percent slopes	Complex	ST
120	Sheek-Archuleta-Rock outcrop complex, 25 to 80 percent slopes	Complex	ST
121	Sheek-Archuleta-Rock outcrop complex, 25 to 80 percent slopes, north aspect	Complex	ST
122	Sheppard fine sand, 1 to 6 percent slopes	Consociation	ED
123	Sideshow silty clay loam, 0 to 3 percent slopes	Consociation	CL
124	Sideshow silty clay loam, 3 to 6 percent slopes	Consociation	CL
125	Sideshow silty clay loam, 6 to 12 percent slopes	Consociation	CL
126	Sideshow-Zigzag complex, 3 to 25 percent slopes	Complex	CL
113	Sharps loam, 6 to 12 percent slopes	Consociation	DE
114	Sharps loam, dry, 6 to 12 percent slopes	Consociation	DE
115	Sharps, dry-Gapmesa complex, 6 to 12 percent slopes	Complex	DE
116	Sharps-Cahona complex, 6 to 12 percent slopes	Complex	DE
117	Sharps-Pulpit complex, 2 to 6 percent slopes	Complex	DE
118	Sharps-Pulpit complex, 6 to 12 percent slopes	Complex	DE
143	Wetherill loam, 1 to 3 percent slopes	Consociation	DE
144	Wetherill loam, 3 to 6 percent slopes	Consociation	DE
145	Wetherill loam, 6 to 12 percent slopes	Consociation	DE
71	Mikett clay loam, saline-sodic, 0 to 3 percent slopes	Consociation	FN
72	Mikett clay loam, 0 to 3 percent slopes	Consociation	FN
73	Mikim clay loam, 1 to 3 percent slopes	Consociation	FN
74	Mikim clay loam, sodic, 0 to 3 percent slopes	Consociation	FN
75	Mikim loam, 3 to 6 percent slopes	Consociation	FN
135	Ustic Torrifluvents, 0 to 3 percent slopes	Consociation	FN
146	Yarts clay loam, 1 to 6 percent slopes	Consociation	FN
147	Yarts fine sandy loam, 1 to 6 percent slopes	Consociation	FN
76	Morefield loam, 1 to 3 percent slopes	Consociation	MVL
77	Morefield loam, 3 to 6 percent slopes	Consociation	MVL
111	Roubideau loam, 1 to 6 percent slopes	Consociation	MVL
3	Arabrab loamy sand, 3 to 9 percent slopes	Consociation	SH
4	Arabrab-Longburn complex, 3 to 15 percent slopes	Complex	SH
30	Falconry gravelly fine sandy loam, 3 to 25 percent slopes	Consociation	SH
31	Farb-Rock outcrop complex, 3 to 12 percent slopes	Complex	SH
42	Gladel-Pulpit complex, 3 to 9 percent slopes	Complex	SH
64	Lazear-Rock outcrop complex, 12 to 65 percent slopes	Complex	SH
68	Longburn-Rock outcrop complex, 10 to 45 percent slopes	Complex	SH
69	Longburn-Rock outcrop complex, 45 to 80 percent slopes	Complex	SH
128	Stephouse-Rock outcrop complex, 3 to 10 percent slopes	Complex	SH
149	Zigzag very channery clay loam, 3 to 25 percent slopes	Consociation	SH
150	Zigzag-Sideshow complex, 25 to 65 percent slopes	Complex	SH
151	Zyme gravelly clay loam, 3 to 12 percent slopes	Consociation	SH
152	Zyme very channery clay loam, 12 to 65 percent slopes	Consociation	SH
5	Archuleta-Sanchez complex, 12 to 65 percent slopes	Complex	ST
6	Argiustolls-Haplustalfs complex, 30 to 80 percent slopes	Complex	ST
7	Argiustolls-Haplustalfs-Rock outcrop complex, 30 to 80 percent slopes	Complex	ST
79	Northrim cobbly loam, 15 to 40 percent slopes	Consociation	ST
80	Ormiston-Beje complex, 5 to 30 percent slopes	Complex	ST
86	Pinacol loam, 12 to 40 percent slopes	Consociation	ST
89	Pramiss very cobbly loam, 6 to 25 percent slopes	Consociation	ST
91	Prater loam, 10 to 25 percent slopes	Consociation	ST
92	Prater-Dolcan complex, 25 to 60 percent slopes	Complex	ST
109	Romberg-Crosscan complex, 6 to 25 percent slopes	Complex	ST

127	Sideslide silty clay loam, 3 to 9 percent slopes	Consociation	CL
128	Stephouse-Rock outcrop complex, 3 to 10 percent slopes	Complex	SH
129	Torriorthents, 12 to 65 percent slopes	Consociation	MC
130	Torriorthents-Badland complex, 25 to 100 percent slopes	Complex	MC
131	Tragmon-Sheek complex, 12 to 25 percent slopes	Complex	ST
132	Typic Argiaquolls, 0 to 3 percent slopes	Consociation	CAL
133	Typic Torriorthents-Rock outcrop complex, 12 to 80 percent slopes	Complex	ST
134	Umbarg-Winner-Tesajo complex, 0 to 2 percent slopes	Complex	AL
135	Ustic Torrifluvents, 0 to 3 percent slopes	Consociation	FN
136	Ustic Torriorthents-Gullied land complex, 1 to 60 percent slopes	Complex	AL
137	Ustorthents, 12 to 65 percent slopes	Consociation	ST
138	Uzacol-Zwicker-Claysprings complex, 3 to 12 percent slopes	Complex	DR
139	Water	Undiff	MC
140	Wauquie very stony loam, 6 to 25 percent slopes	Consociation	ST
141	Wauquie-Dolcan complex, 6 to 25 percent slopes	Complex	ST
142	Wauquie-Dolcan-Rock outcrop complex, 25 to 80 percent slopes	Complex	ST
143	Wetherill loam, 1 to 3 percent slopes	Consociation	DE
144	Wetherill loam, 3 to 6 percent slopes	Consociation	DE
145	Wetherill loam, 6 to 12 percent slopes	Consociation	DE
146	Yarts clay loam, 1 to 6 percent slopes	Consociation	FN
147	Yarts fine sandy loam, 1 to 6 percent slopes	Consociation	FN
148	Zau stony loam, 9 to 25 percent slopes	Consociation	ST
149	Zigzag very channery clay loam, 3 to 25 percent slopes	Consociation	SH
150	Zigzag-Sideshow complex, 25 to 65 percent slopes	Complex	SH
151	Zyme gravelly clay loam, 3 to 12 percent slopes	Consociation	SH
152	Zyme very channery clay loam, 12 to 65 percent slopes	Consociation	SH

110	Romberg-Crosscan-Rock outcrop complex, 25 to 80 percent slopes	Complex	ST
119	Sheek-Archuleta complex, 6 to 25 percent slopes	Complex	ST
120	Sheek-Archuleta-Rock outcrop complex, 25 to 80 percent slopes	Complex	ST
121	Sheek-Archuleta-Rock outcrop complex, 25 to 80 percent slopes, north aspect	Complex	ST
131	Tragmon-Sheek complex, 12 to 25 percent slopes	Complex	ST
133	Typic Torriorthents-Rock outcrop complex, 12 to 80 percent slopes	Complex	ST
137	Ustorthents, 12 to 65 percent slopes	Consociation	ST
140	Wauquie very stony loam, 6 to 25 percent slopes	Consociation	ST
141	Wauquie-Dolcan complex, 6 to 25 percent slopes	Complex	ST
142	Wauquie-Dolcan-Rock outcrop complex, 25 to 80 percent slopes	Complex	ST
148	Zau stony loam, 9 to 25 percent slopes	Consociation	ST
22	Claysprings very stony clay loam, 12 to 65 percent slopes	Consociation	DR
106	Rizno-Littlenan-Bodry association, 3 to 50 percent slopes	Association	DR
138	Uzacol-Zwicker-Claysprings complex, 3 to 12 percent slopes	Complex	DR
70	Mack fine sandy loam, 0 to 6 percent slopes	Consociation	ED
100	Recapture fine sandy loam, 0 to 6 percent slopes	Consociation	ED
101	Recapture sandy loam, 0 to 6 percent slopes	Consociation	ED
105	Rizno-Gapmesa complex, 3 to 9 percent slopes	Complex	ED
107	Rizno-Ruinpoint-Rock outcrop complex, 1 to 15 percent slopes	Complex	ED
122	Sheppard fine sand, 1 to 6 percent slopes	Consociation	ED
28	Dam	Consociation	MC
87	Pits	Consociation	MC
108	Rock outcrop	Consociation	MC
129	Torriorthents, 12 to 65 percent slopes	Consociation	MC
130	Torriorthents-Badland complex, 25 to 100 percent slopes	Complex	MC
139	Water	Undifferentiated group	MC

Supplementary Table 3. Elevations, locations and total N values in top 50 cm of study area soils

Sample No.	Ele (m)		UTM Cooridinates		Total N (50 cm) (%N)
Cool eolian soils (loess) (9/14/2011)					
CE-1	2390	12S	695146	4183781	0.097
CE-2	2391	12S	695184	4183755	0.098
CE-3	2383	12S	695186	4183727	0.147
CE-4	2384	12S	695159	4183729	0.114
CE-5	2382	12S	695141	4183718	0.101
CE-6	2382	12S	695129	4183676	0.104
CE-7	2328	12S	695290	4182230	0.074
CE-8	2330	12S	695331	4182228	0.088
CE-9	2335	12S	695379	4182235	0.119
CE-10	2336	12S	695386	4182199	0.107
CE-11	2339	12S	695415	4182150	0.118
CE-12	2344	12S	695461	4182145	0.068
CE-13	2322	12S	694732	4181707	0.103
CE-14	2319	12S	694725	4181745	0.095
CE-15	2321	12S	694731	4181817	0.110
CE-16	2318	12S	694650	4181857	0.097
CE-17	2317	12S	694661	4181803	0.111
CE-18	2320	12S	694700	4181763	0.092
CE-19	2306	12S	694252	4181544	0.077
CE-20	2308	12S	694313	4181499	0.110
CE-21	2309	12S	694362	4181513	0.099
CE-22	2311	12S	694386	4181567	0.093
CE-23	2310	12S	694432	4181583	0.090
CE-24	2311	12S	694468	4181600	0.081
CE-25	2278	12S	693090	4181865	0.094
CE-26	2279	12S	693062	4181915	0.112
CE-27	2277	12S	693003	4181918	0.093
CE-28	2279	12S	692955	4181941	0.103
CE-29	2280	12S	692934	4181991	0.080
CE-30	2281	12S	693104	4181953	0.086
Deep eolian soils (loess) (9/14/2011)					
DE-1	2064	12S	684388	4141946	0.076
DE-2	2063	12S	694408	4141967	0.093
DE-3	2063	12S	694437	4141989	0.108
DE-4	2065	12S	694453	4141985	0.072
DE-5	2064	12S	694441	4141945	0.079

DE-6	2060	12S	693971	4141889	0.082
DE-7	2063	12S	694010	4141873	0.056
DE-8	2065	12S	694013	4141843	0.053
DE-9	2063	12S	693989	4141818	0.039
DE-10	2066	12S	693964	4141838	0.027
DE-11	2044	12S	692540	4141777	0.037
DE-12	2045	12S	692539	4141810	0.035
DE-13	2045	12S	692530	4141847	0.035
DE-14	2045	12S	692541	4141898	0.053
DE-15	2043	12S	692488	4141879	0.052
DE-16	1959	12S	688104	4140844	0.065
DE-17	1959	12S	688132	4140865	0.028
DE-18	1958	12S	688167	4140892	0.044
DE-19	1959	12S	688214	4140889	0.040
DE-20	1959	12S	688270	4140891	0.022
DE-21	1975	12S	689176	4141078	0.036
DE-22	1975	12S	689216	4141089	0.053
DE-23	1977	12S	689249	4141099	0.053
DE-24	1977	12S	689286	4141097	0.066
DE-25	1980	12S	689313	4141070	0.038
Alluvial soils (9/15/2011)					
AL-1	1939	12S	721913	4136569	0.049
AL-2	1939	12S	721946	4136575	0.036
AL-3	1941	12S	721978	4136623	0.037
AL-4	1940	12S	722041	4136661	0.057
AL-5	1941	12S	722100	4136699	0.045
AL-6	1938	12S	722168	4136663	0.080
AL-7	1937	12S	722239	4136646	0.066
AL-8	1935	12S	722315	4136665	0.095
AL-9	1935	12S	722347	4136739	0.055
AL-10	1936	12S	722384	4136826	0.048
AL-11	1936	12S	722432	4136883	0.040
AL-12	1937	12S	722477	4136951	0.057
AL-13	1936	12S	722510	4136995	0.056
AL-14	1935	12S	722479	4137059	0.108
AL-15	1936	12S	722469	4137123	0.151
AL-16	1934	12S	722604	4136801	0.089
AL-17	1935	12S	722566	4136748	0.064
AL-18	1934	12S	722530	4136655	0.085
AL-19	1933	12S	722534	4136586	0.071

AL-20	1936	12S	722607	4136593	0.098
AL-21	1940	12S	722873	4136627	0.083
AL-22	1941	12S	722927	4136563	0.112
AL-23	1942	12S	722988	4136537	0.092
AL-24	1944	12S	723050	4136519	0.079
AL-25	1938	12S	723109	4136517	0.094
Clay soils (derived from Mancos Shale) (9/15/2011)					
CL-1	2032	12S	727941	4137390	0.068
CL-2	2035	12S	727990	4137447	0.078
CL-3	2036	12S	728043	4137498	0.080
CL-4	2039	12S	728115	4137479	0.079
CL-5	2042	12S	728177	4137447	0.074
CL-6	2044	12S	728249	4137434	0.071
CL-7	2046	12S	728306	4137419	0.088
CL-8	2048	12S	728349	4137384	0.075
CL-9	2049	12S	728408	4137364	0.058
CL-10	2052	12S	728474	4137351	0.080
CL-11	2053	12S	728471	4137296	0.094
CL-12	2052	12S	728442	4137235	0.093
CL-13	2052	12S	728428	4137181	0.099
CL-14	2052	12S	728404	4137142	0.100
CL-15	2055	12S	728421	4137103	0.102
CL-16	2059	12S	728443	4137045	0.079
CL-17	2059	12S	728444	4136969	0.108
CL-18	2058	12S	728441	4136902	0.064
CL-19	2057	12S	728391	4136937	0.052
CL-20	2054	12S	728344	4136981	0.086
CL-21	2038	12S	727566	4137287	0.117
CL-22	2037	12S	727537	4137326	0.111
CL-23	2038	12S	727500	4137273	0.102
CL-24	2038	12S	727447	4137226	0.075
CL-25	2037	12S	727380	4137226	0.085
Alluvial fan soils (9/16/2011)					
FN-1	2032	12S	725493	4133115	0.152
FN-2	2029	12S	725437	4133074	0.107
FN-3	2027	12S	725371	4133011	0.132
FN-4	2024	12S	725296	4132981	0.117
FN-5	2020	12S	725192	4132880	0.108
FN-6	2019	12S	725133	4132827	0.107

FN-7	2019	12S	725066	4132769	0.090
FN-8	2019	12S	724965	4132685	0.104
FN-9	2018	12S	724895	4132654	0.104
FN-10	2019	12S	724820	4132563	0.098
FN-11	2021	12S	724761	4132505	0.096
FN-12	2021	12S	724716	4132460	0.131
FN-13	2019	12S	724662	4132404	0.087
FN-14	2022	12S	724607	4132350	0.084
FN-15	2023	12S	724556	4132294	0.172
FN-16	2026	12S	724597	4132229	0.106
FN-17	2026	12S	724649	4132250	0.098
FN-18	2027	12S	724705	4132271	0.111
FN-19	2028	12S	724754	4132296	0.093
FN-20	2027	12S	724808	4132341	0.111
FN-21	2027	12S	724852	4132366	0.112
FN-22	2026	12S	724907	4132401	0.093
FN-23	2027	12S	724959	4132420	0.081
FN-24	2026	12S	724992	4132475	0.116
FN-25	2022	12S	724955	4132525	0.115
Mesa Verde Chapin Mesa burned loessic soils (9/23/2008)					
Elevation of Mesa Verde ranges between 2440 and 2560 m					
CMB1	2168	13S	190726	4122547	0.081
CMB2	2194	13S	190346	4123254	0.072
CMB3	2192	13S	190247	4123104	0.054
CMB4	2213	13S	190188	4123828	0.037
CMB5	2213	13S	190111	4123896	0.055
CMB6	2247	13S	189919	4124662	0.056
CMB7	2245	13S	189848	4124658	0.058
CMB8	2420	13S	189405	4128464	0.097
CMB9	2425	13S	189357	4128533	0.124
CMB10	2134	13S	191109	4121023	0.058
Mesa Verde Chapin Mesa unburned loessic soils (9/23/2008)					
CMUB1	2282	13S	189217	4125602	0.056
CMUB2	2282	13S	189197	4125587	0.067
CMUB3	2313	13S	189014	4126366	0.085
CMUB4	2346	13S	189173	4127131	0.078
CMUB5	2352	13S	188952	4127145	0.062
CMUB6	2366	13S	189161	4127603	0.081
CMUB7	2379	13S	189194	4127782	0.101
CMUB8	2085	13S	192036	4118724	0.083

CMUB9	2089	13S	191899	4118997	0.247
CMUB10	2112	13S	191725	4119893	0.049
CMUB11	2125	13S	191697	4120465	0.051
CMUB12	2151	13S	190669	4121688	0.081
Mesa Verde Wetherill Mesa burned loessic soils (9/22/2008)					
WM34-1	2273	13S	185321	4124962	0.038
WM34-2	2274	13S	185306	4124962	0.073
WM34-3	2274	13S	185300	4124996	0.032
WM34-4	2277	13S	185327	4125021	0.031
WM34-5	2276	13S	185314	4125008	0.030
WMB1	2150	13S	186757	4120758	0.044
WMB2	2150	13S	186768	4120717	0.046
WMB3	2150	13S	186795	4120675	0.042
WMB4	2149	13S	186794	4120632	0.062
WMB5	2149	13S	186798	4120593	0.080
Mesa Verde Wetherill Mesa unburned loessic soils (9/22/2008)					
WMOG1	2144	13S	186960	4120757	0.054
WMOG2	2146	13S	186942	4120752	0.054
WMOG3	2147	13S	186921	4120763	0.054
WMOG4	2148	13S	186903	4120741	0.036
WMOG5	2149	13S	186873	4120759	0.038
WMOG6	2149	13S	186859	4120510	0.046
WMOG7	2149	13S	186835	4120493	0.051
WMOG8	2148	13S	186885	4120491	0.037
WMOG9	2146	13S	186916	4120474	0.054
WMOG10	2145	13S	186943	4120479	0.050
Mesa Verde Morefield Valley alluvial soils (9/23/2008)					
MV1	2192	13S	197478	4126552	0.098
MV2	2194	13S	197539	4126641	0.105
MV3	2194	13S	197632	4126748	0.135
MV4	2194	13S	197811	4126982	0.091
MV5	2202	13S	197859	4127175	0.116
MV6	2201	13S	197791	4127307	0.107
MV7	2206	13S	197773	4127518	0.136
MV8	2212	13S	197731	4127802	0.276
MV9	2235	13S	197631	4128553	0.203
Mesa Verde Chapin Mesa side-valley terrace alluvial soils (9/23/2008)					
CMT1	2140	13S	190936	4122347	0.055
CMT2	2140	13S	190935	4122345	0.054
CMT3	2143	13S	190929	4122338	0.068

CMT4	2144	13S	190926	4122334	0.081
CMT5	2145	13S	190918	4122330	0.072
Bandelier transect soils (7/14/2009)					
BA-1	2323	13S	377088	3966322	0.029
BA-2	2309	13S	378140	3966258	0.048
BA-3	2261	13S	379072	3966234	0.026
BA-4	2251	13S	379746	3965649	0.061
BA-5	2218	13S	380746	3965561	0.048
BA-6	2196	13S	381400	3964955	0.072
BA-7	2166	13S	382116	3964216	0.068
BA-8	2140	13S	382630	3963549	0.058
BA-9	2106	13S	383396	3962853	0.055
BA-10	2034	13S	384596	3962148	0.036
BA-11	2029	13S	384712	3961711	0.060
BA-12	2019	13S	385019	3961264	0.062
BA-13	2011	13S	385072	3961283	0.061
BA-14	1997	13S	385436	3960505	0.034
BA-15	1860	13S	384913	3960443	0.032
BA-16	1860	13S	384744	3960624	0.058
Janice Day Corn Field at Hopi (9/28/2011)					
JD-1	1670	12S	543356	3954409	0.013
JD-2	1670	12S	543334	3954453	0.007
JD-3	1670	12S	543319	3954430	0.005
JD-4	1670	12S	543358	3954363	0.032
JD-5	1670	12S	543374	3954378	0.040
Zuni fields (8/19-20/2008)					
BA1A	2080	13S	169941	3897512	0.053
BA1B	2077	13S	169597	3897352	0.072
BC1A	2089	13S	167660	3896512	0.105
BC1B	2085	13S	167799	3896480	0.058
BC5A	2030	13S	163569	3899993	0.082
BC5B	2030	13S	163536	3899945	0.060
BU1	2097	13S	167944	3897509	0.081
WE1	2086	13S	168335	3897416	0.048
BU3A	2091	13S	167717	3896426	0.053
BU3B	2092	13S	167700	3896434	0.079
NA2A	2066	13S	172802	3907289	0.082
NA2B	2064	13S	172883	3907293	0.073
NA3A	2072	13S	170807	3906877	0.074
NA3B	2070	13S	170794	3906683	0.123
NC1A	2081	13S	175495	3908770	0.093
NC1B	2084	13S	175393	3908685	0.057
NC2A	2074	13S	175182	3906713	0.069
NC2B	2074	13S	175525	3906800	0.054

NC3A	2076	13S	175101	3908723	0.122
NC3B	2075	13S	175065	3908757	0.120
PA1A	2050	13S	172034	3892391	0.089
PA1B	2051	13S	172147	3892493	0.082
PA2A	2061	13S	171871	3891061	0.056
PA2B	2058	13S	171881	3891215	0.025
PC1A	2072	13S	172229	3890478	0.063
PC1B	2067	13S	172196	3890622	0.093
PC2A	2060	13S	171100	3891505	0.061
PC2B	2055	13S	171195	3891732	0.072
PC3A	2044	13S	170965	3893125	0.119
PC3B	2044	13S	171092	3893236	0.105
Chaco Corridor					
Chaco Canyon					
SG08-1	1881	13S	232270	3993416	0.062
SG08-2	1870	13S	232419	3993708	0.135
SG08-3	1870	13S	232633	3994201	0.111
WR08-1	1882	13S	235012	3993138	0.022
WR08-2	1881	13S	235120	3993228	0.026
PB08-1	1851	13S	231081	3996239	0.028
PB08-2	1860	13S	231191	3996043	0.054
CC08-1	1866	13S	231454	3995909	0.044
KN08-1	1891	13S	237241	3992489	0.029
MB08-1	1888	13S	236558	3993668	0.056
MB08-2	1881	13S	236428	3993593	0.075
MB08-3	1879	13S	236228	3993440	0.027
LH08-1	1876	13S	234490	3994323	0.043
GW08-1	1914	13S	242421	3993387	0.073
GW08-2	1909	13S	241943	3993347	0.084
GW08-3	1906	13S	240729	3992502	0.096
FB08-1	1887	13S	237470	3990851	0.016
FB08-2	1886	13S	237235	3990990	0.047
Rio Chaco					
KK08-1	1851	13S	222941	3991737	0.035
KK08-2	1846	13S	223294	3991988	0.044
KK08-3	1843	13S	223627	3991998	0.049
KK08-4	1841	13S	223660	3992230	0.047
KK08-5	1840	13S	223653	3992466	0.037
CDR08-1	1821	13S	222813	3997921	0.008
CDR08-2	1822	13S	223064	3998237	0.005
CDR08-3	1822	13S	223155	3998557	0.029
CDR08-4	1820	13S	222857	3998204	0.006
GB08-1	1687	13S	185266	4008780	0.064
GB08-2	1688	13S	185755	4008256	0.085
GB08-3	1691	13S	186624	4007758	0.057
GB08-4	1697	13S	187908	4007552	0.075

GB08-5	1706	13S	189163	4007618	0.074
IC08-1	1745	13S	197787	4001989	0.021
WC08-1	1710	13S	190263	4007951	0.070
WC08-2	1722	13S	191328	4007140	0.059
WC08-3	1736	13S	192110	4006315	0.070
EC08-1	1961	13S	251859	3984943	0.042
EC08-2	1950	13S	251960	3985359	0.028
EC08-3	1942	13S	252123	3985958	0.027
PP08-1	1970	13S	260213	3986632	0.060
PP08-2	1976	13S	260419	3986254	0.035
PP08-3	1970	13S	261195	3985638	0.067
PP08-4	1974	13S	260819	3985218	0.080
PP08-5	1981	13S	259731	3983069	0.070
Chuska Slope					
SS08-1	1750	13S	162718	4016234	0.028
SS08-2	1740	13S	163406	4016321	0.055
TGHBM08-1	1855	13S	155749	4015408	0.022
TGHBM08-2	1840	13S	156275	4015921	0.022
TGHBM08-3	1871	13S	155047	4015315	0.047
CH08-1	1776	13S	159663	4014143	0.028
CH08-2	1761	13S	160379	4014124	0.043
CH08-3	1756	13S	161078	4014844	0.034
CTW08-1	1697	13S	166611	4022354	0.030
CTW08-2	1714	13S	164198	4022355	0.039
CTW08-3	1693	13S	167329	4023043	0.088
CTW08-4	1691	13S	167676	4023074	0.043
CTW08-5	1630	13S	178972	4029615	0.038
CTW08-6	1623	13S	178469	4029138	0.082

Suplementary Table 4. Elevation, mean summer T, annual T, GDD, and FFD for Southwest Colorado weather stations

	Ele (m)	Avg JJAS T (ºC)	1σ	Avg Ann T	1σ	Avg GDD	1σ	FFD 90%P	120 FFD P	>115 FFD (%)
Hovenweep	1597	21.8	0.9	10.5	0.53	1756	146	125	>90	94
Cortez	1888	19.6	0.8	9.07	0.49	1366	140	110	59	73
Ignacio	1960	17.6	0.9	7.52	0.88	1040	131	80	18	22
Durango	2030	17.4	0.8	8.33	0.47	1011	112	88	32	36
Yellow Jacket	2091	19.0	1.0	8.49	0.78	1285	167	116	78	88
Mesa Verde	2159	19.8	1.0	9.52	0.68	1421	181	122	>90	92
Vallecito	2332	15.5	1.0	5.78	0.75	738	126	85	18	21
Rico	2687	12.2	0.7	3.67	0.64	336	67	28	0	0

FFD 90%P indicates 90% probability of those number of FFD between 0ºC in spring and 0^0Cn in autumn

120 FFD P indicates the probability (%) of achieving 120 FFD

>115 FFD (%) indicates the percent of the time that the site has achieved greater than 115 FFD